



Assessment of future overheating conditions in Canadian cities using a reference year selection method

Jiwei Zou^{a,*}, Abhishek Gaur^b, Liangzhu (Leon) Wang^a, Abdelaziz Laouadi^b, Michael Lacasse^b

^a Centre for Zero Energy Building Studies, Department of Building, Civil and Environmental Engineering, Concordia University, Montreal, Canada

^b Construction Research Centre, National Research Council Canada, 1200 Montreal Road, K1A 0R6, Ottawa, Ontario, Canada



ABSTRACT

Climate change has led to prolonged, more frequent, intense, and severe extreme weather events, such as summertime heatwaves, creating many challenges on the economy and society and human health and energy resources. For example, the 2010 and 2018 heatwave in Quebec, Canada, resulted in about 280 and 93 heat-related deaths, and there were around 500 fatalities due to overheated indoor environments in 2021 around entire Canada. Therefore, it is imperative to understand and evaluate the overheating conditions in buildings, for which selecting suitable future reference weather data under climate change is one of the first critical steps. This study evaluated a reference year selection method in terms of typical and extreme reference years based on future climate datasets to assess both outdoor and indoor overheating in the future. The future climate data were collected from the Coordinated Regional Downscaling Experiment (CORDEX) program. Three Canadian cities (Montreal, Toronto, Vancouver) were selected for the overheating evaluation during three selected periods (2001–2020, 2041–2060, 2081–2100). The CORDEX climate projections were first bias-corrected by the multivariate quantile mapping correction method with the observational data. Then, the typical and extreme reference year data were generated as well as climate data from the design summer year for comparison. The performance of the reference year selection method was evaluated by comparing the maximum, minimum, and average overheating hours for the 20-years data of each period. This study demonstrates that the multivariate quantile mapping bias correction method can improve the reliability of future climate data making it one of the most important steps for any future weather projection study. Besides, the reference year selection method could efficiently capture maximum and minimum monthly overheating hours providing the upper and lower boundary of possible outdoor and indoor overheating conditions. In contrast, neither the severest nor the typical monthly outdoor and indoor overheating conditions could be predicted by the design summer year method. Finally, owing to the effects of climate change, average monthly overheating hours normally increase by around one time (from 50% to 150%) until the mid-term future (2041–2060) and by around two to three times (even up to nine times for some scenarios) during the long-term future (2081–2100).

1. Introduction

Due to greenhouse gas emissions, the global climate system has been significantly affected, which resulted in more intense and frequent extremely hot outdoor conditions in recent years all around the world [1–5]. Human daily life was affected by these extreme weather conditions in diverse aspects, including economy, health, society, energy, and infrastructure systems [1,6–8]. In 2003, Europe experienced one of the hottest summers in the past 500 years with more than 30000 deaths [9, 10] and record-high temperatures of 20–30% above the average of June to mid-August [11]. In the Netherlands, around 2000 heat-related deaths occurred during summer with a maximum temperature of 35 °C [3]. The 2010 heatwave in Quebec, Canada, resulted in a significant increase of 33% in the crude death rate (about 280 extra deaths) [12] and the 2018 heatwave in Quebec caused 93 deaths. Although both outdoor and indoor overheating has garnered much attention during recent years in Canada, the most recent heatwave in 2021 still caused

about 500 deaths across the country [13]. As a consequence of global warming, the frequencies, magnitudes, and intensities of heat events in Canada, and indeed around the globe, are expected to keep increasing in the future [14,15]. It is expected that the deadly heatwaves would occur about 60 days annually in the mid-latitudes and affect 48%~74% of the world's population by 2100 [16].

Building environments provide shelters from weather extremes and ensure the quality of life for residents [17,18]. This has been greatly challenged in recent decades [19,20]. Although there are limited studies on the epidemiological evidence that high-temperature exposures indoors contribute to adverse health effects [21,22], it could be self-evident that the above-mentioned heat-related deaths were not only caused by the intolerable outdoor conditions but also the inability of buildings to moderate extreme temperatures indoors [23]. It has also been reported that exposure to elevated indoor temperatures reduces the ability of a human body to recover from outdoor heat stress [24,25], causing sleep fragmentation [26,27], poor work performance [28], and possibly impairing the mental health [29,30].

* Corresponding author.

E-mail address: jiwei.zou@mail.concordia.ca (J. Zou).

Abbreviation	
GCMs	Global Climate Models
RCP	Representative Concentration Pathway
SSP	Shared Socioeconomic Pathway
TMY	Typical Meteorological Year
TDY	Typical Downscaled Year
ECY	Extreme Cold Year
EWY	Extreme Warm Year
DSY	Design Summer Year
RCM	Regional Climate Model
CORDEX	Coordinated Regional Downscaling Experiment
MBCn	Multivariate Bias Correction Algorithm
CDF	Cumulative Distribution Function
tas	Air Temperature
rsds	Solar Radiation
hurs	Relative Humidity
sfcWind	Wind Velocity at ground surface
MPI	MPI-ESM-LR
NCC	NCC-NorESM1-M
MOHC	MOHC-HadGEM2-ES
Max	Maximum value of monthly 20-years overheating hours
Ave	Average value of monthly 20-years overheating hours
Min	Minimum value of monthly 20-years overheating hours

Free-running residential buildings are one of the most vulnerable building types to the risks of overheating [31]. There have been many studies assessing indoor conditions of buildings across various countries and climate zones, such as the United Kingdom [32–34], the Netherlands [3,35,36], Sweden [37,38], and Canada [39–41] in respect to temperate climates, Honduras [42], Taiwan [43], and Hong Kong [2, 44] for tropical and subtropical climates. Most previous studies focused on existing overheating conditions [2,33,38,42,45]. In contrast, increasing attention started towards the future overheating scenarios [3, 37,44], and the prediction of future overheating effects relying on building simulation models with current and future projected climatic conditions.

An essential part of future overheating assessments is to prepare projected future climate files as inputs to a building simulation model. They are usually from global climate models (GCMs), including an atmospheric model, ocean model, land surface scheme, and a sea ice model [46]. However, the major challenges of using GCMs are various existing climate models and multiple greenhouses gas emission scenarios creating many options and complexities for users to choose from. For the Coupled Model Intercomparison Project Phase 5 (CMIP5), forty GCMs from 20 research groups were proposed and publicly available [47]. The Intergovernmental Panel on Climate Change (IPCC) has four Representative Concentration Pathways (RCPs) that represent different future greenhouse gas emission scenarios, including RCP 2.6, RCP 4.5, RCP 6.0, and RCP 8.5. More recently, led by the IPCC, the energy modeling community developed a new set of emission scenarios driven by different socioeconomic assumptions, the so-called ‘Shared Socio-economic Pathways’ (SSPs). A number of these SSP scenarios have been selected to drive climate models as part of the Coupled Model Intercomparison Projects 6 (CMIP6). The previous RCP scenarios have been updated in CMIP6 in the form of SSP1-2.6, SSP2-4.5, SSP4-6.0, and SSP5-8.5, each of which results in similar 2100 radiative forcing levels as their predecessors in RCPs. Several new scenarios were also applied in CMIP6, such as SSP1-1.9, SSP4-3.4, SSP5-3.4OS, and SSP3-7.0, to take into account more socioeconomic drivers. Such a large number of climate models and RCP scenarios complicate the process of applying their different combinations to one specific assessment and enormous computational costs. Moreover, a building overheating assessment for future projected years is expected to cover a long-term period of at least 20–30 years [46], which results in high computational costs when evaluating every year. Therefore, one of the computationally effective solutions is to select a few reference years as the subsets of the long-term time-series climates while encompassing the uncertainties associated with future climate projections.

Reference years are one year (or a few years) prepared from the climate time series to capture aspects of interest from the long-term datasets. For building energy applications, the typical meteorological year (TMY) defined by Hall et al. [48] is often used by combining multiple typical meteorological months (TMM). TMY was widely applied to evaluating building energy performance [49–54] as well as

the overheating assessment [2,49–56]. In comparison, Typical reference year (TRY), Weather Year for Energy Calculations (WYEC), and International Weather Year for Energy Calculations (IWEC) were developed by the American Society of Heating, Refrigerating, and Air-conditioning Engineers (ASHRAE). The test reference year from Hui and Lok [57] and typical meteorological year 2 (TMY2) from the National Solar Radiation Data Base (NSRDB) [58] were intended to capture typical, or average, aspects of climatic variables of the long-term datasets [59–61].

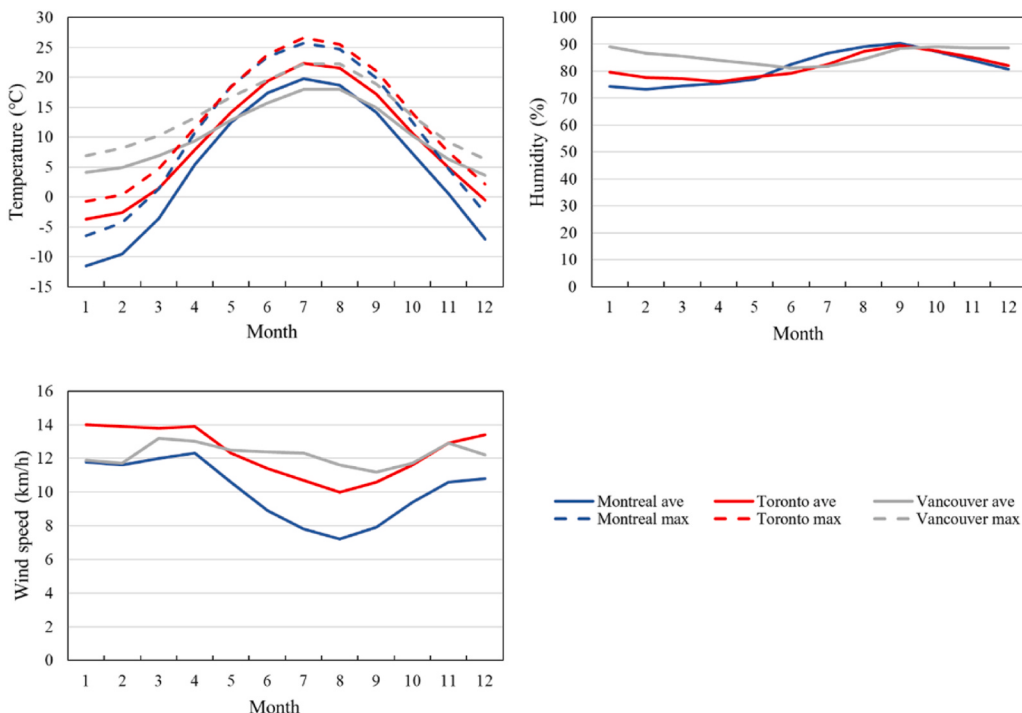
There are also reference year methods for building overheating assessments, the intention of which is to capture extreme summer conditions from long-term data as the reference datasets, like the design summer year (DSY) from Levermore and Parkinson [62], actual meteorological year (AMY) from Hong et al. [63], summer reference year from Jentsch et al. [64]. For a cold climate, such as Canada, several studies have focused on the overheating assessment in different cities [19,39,41,45,65]. Baba and Ge [39] evaluated the performance of existing buildings under a current extreme year and projected future climates. Their results showed that the thermal conditions of a single-family detached house built in 1964 and 1990 are more comfortable than the house built to meet the current National Energy Code of Canada for Buildings (NECB), and the overheating risk of Canadian buildings will be increased in the future. In a recent study, Chang et al. [19] evaluated the external overheating within the urban areas of Ottawa and Montreal by Weather Research and Forecasting (WRF) simulations with two resolutions (1 km and 25 km). Besides, the WRF simulation data were then used for the indoor overheating assessment by EnergyPlus simulations. It was shown that the 1-km grid resolution is essential for assessing indoor overheating conditions because the 25-km resolution could lead to an underprediction of the overheating hours in about 95% of the urban grids within either of these two cities. Studies from Laouadi [45,65,66] developed a new reference year method called reference summer weather years (RSWY) to evaluate indoor overheating. This method includes generating historical climate data, developing a heat stress metric for the definition, and characterizing heat events. A modified Standard Effective Temperature (t-SET) considering both environmental and psychological factors was used to generate RSWY for selected Canadian cities. This method was also applied to evaluate future climate change impacts on indoor overheating [40].

Recently, Nik [46] developed an approach for selecting reference years for climate change impact assessment on buildings where three reference years: typical downscaled year (TDY), extreme cold year (ECY), and extreme warm year (EWY), were selected to capture the typical, coldest and warmest conditions within a climate time-series. This method aims at selecting the limited number of hourly weather data sets out of regional climate models (RCMs) without neglecting the climate uncertainties, extremes, and variations in different time scales without weighting weather parameters in time series. The selected three reference years are found to efficiently capture the range of climatic projections and building energy response from an ensemble of regional

Table 1

Information of three selected Canadian cities.

City	Latitude and longitude	Elevation above sea level (m)	City Area (km ²)	Population density (person/km ²)	Climate	Prevailing wind direction
Montreal	45°30'N 73°33'W	36	431.5	4828.3	Semi-continental	West
Toronto	43°44'N 79°22'W	76.5	630.2	4434.1	Semi-continental	West
Vancouver	49°15'N 123°06'W	2	115.2	5749.9	Western maritime	East

**Fig. 1.** Climatic variables of three Canadian cities from 1981 to 2010.

climate projections. The approach has since been applied in a wide range of studies to prepare reference datasets for building energy and building hygrothermal applications [67–70].

More recently, Nik's method is also applied to the future projected changes in indoor thermal comfort and degree-days evaluation of a European city [71]. It is found that cooling degree days increase by 45% for the typical weather conditions and even up to 500% for an extreme warm July from one 30-year period to another. According to their study, the annual overheating hours can increase by up to 140% in the future time under extreme summer months in the city. In this study, the suitability of Nik [44] method towards selecting typical and extreme reference years for indoor and outdoor overheating applications is evaluated over three Canadian cities. This study, therefore, evaluates the method in an overheating context, which is a relatively less explored area of investigation of the method in the past. At the same time, the evaluation is performed over Canadian cities which have different climates than European cities over which previous overheating study [67] with the method has been performed.

The study is described in the following sections. Section 2 provides detailed descriptions of the tasks and workflow process of the study and includes the locations and period of time of interest, the collection of climate data, methods of data processing, building model configurations, and overheating criteria. Results and discussions of data processing, as well as the outdoor and indoor overheating conditions, are reported in Section 3, and the conclusions are provided in Section 4.

2. Methodology

The following steps were conducted to select reference years for the three Canadian cities in an overheating context, and evaluate future projected changes in the overheating of buildings in these locations:

Step one Collection of observational and climate model simulation data (details described in Section 2.2):

The observations were collected from the airport locations for each city and for the time period of 1998–2017 from the CWEEDS database (hereafter referred to as observational time-period). The three sets of regional climate projections were collected from the Coordinated Regional Downscaling Experiment (CORDEX) program for the observational, contemporary, mid-term future, and long-term future time periods and for the grids encompassing the airport locations of the three cities.

Step two Bias correction of climate model simulations (details described in Section 2.3 and 3.1):

The regional climate model data were used to calibrate the multivariate bias correction algorithm (MBCn) bias-correction function, which was then used to prepare bias-corrected climate simulations for the contemporary, mid-term future, and long-term future time periods.

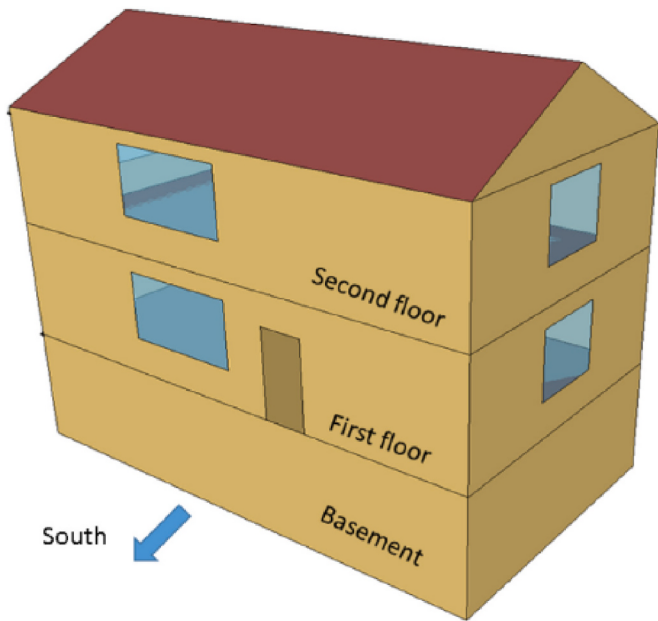


Fig. 2. Archetype of the single-detached house [45].

Table 2
Characteristics of construction practice of the single house building [45].

Envelope	2015 construction practice [106]
Roof	Asphalt shingles with attic insulation ($8.2 \text{ Km}^2/\text{W}$)
Walls	Wood stud with Vinyl cladding ($4.5 \text{ Km}^2/\text{W}$)
Basement wall	Insulated concrete ($1.7 \text{ Km}^2/\text{W}$)
Basement slab	Insulated concrete ($1.6 \text{ Km}^2/\text{W}$)
Windows with wooden frames	Double clear with low- ϵ ($U = 1.58 \text{ W}/(\text{m}^2\text{K})$); Visible transmittance = 73%; Solar heat gain coefficient = 0.67; Window to wall ratio = 15%

Step three Preparation of typical and extreme climate datasets (details described in Section 2.4 and 3.2):

The typical downscaled year (TDY), extreme warm year (EWY), and extreme cold year (ECY) were prepared for the three time periods. In addition, the Design Summer Year (DSY) was selected for the same periods.

Step four Building simulations with current and future projected climate (details described in Section 2.5):

The indoor environment in the single-detached home when exposed to the climate in contemporary, mid-term future, and long-term future time periods were simulated using EnergyPlus simulation software.

Step five Assessment of future outdoor and indoor overheating (describe in Section 3.3):

Future overheating assessment in the cities was performed by comparing the overheating conditions in the mid-term and long-term future to those of the contemporary time period.

2.1. The region and time-periods of interest

Three Canadian cities were selected for the overheating assessment in this study, including Montreal (Quebec), Toronto (Ontario), and Vancouver (British Columbia). These three cities were, in 2016, the three largest urban agglomerations, by population, in Canada [72]. Demographic and geographic details of these three cities are provided in Table 1. For the overheating evaluation, three time periods: contemporary (2001–2020), mid-term future (2041–2060), and long-term future (2081–2100) are considered. Fig. 1 shows the average monthly summary of daily observations of temperature, humidity, and wind speed for the three cities collected from Environment and Climate Change Canada (ECCC) [73].

The daily average (solid line) and daily maximum (dash line) temperature over 1981–2010 are reported in Fig. 1. The average

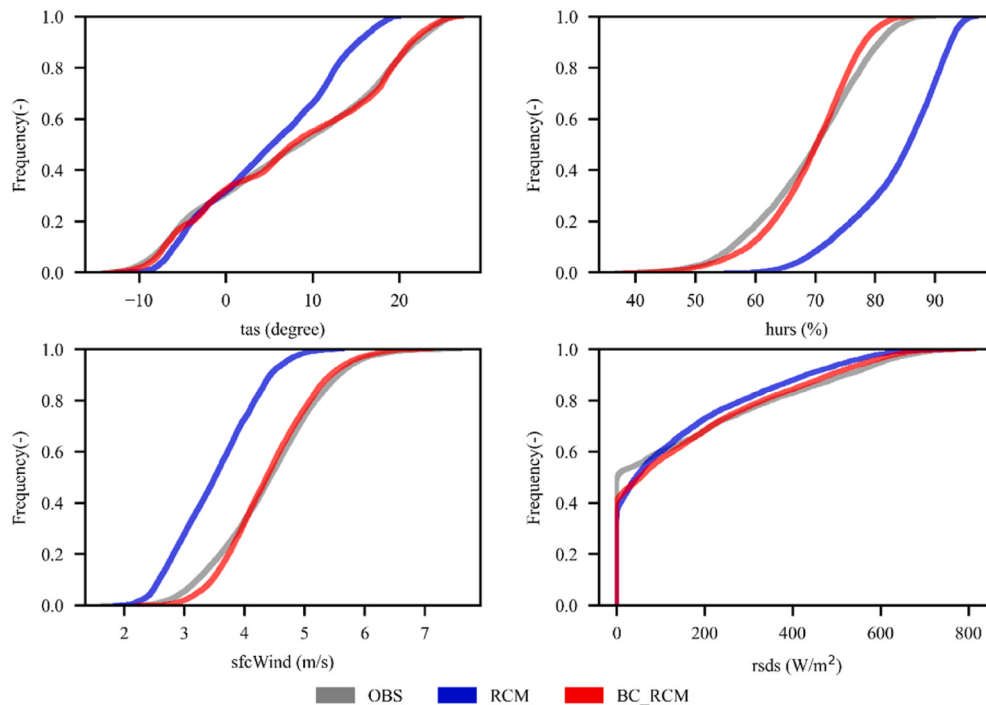


Fig. 3. Cumulative distribution function comparison of observational, raw RCM, and bias-corrected RCM data of dry-bulb air temperature (tas), relative humidity (hurs), wind speed (sfcWind), and global solar radiation (rsds) (City: Montreal; GCM: MPI-M-MPI-ESM-LR; Time periods: 1998–2017).

Table 3

Selected years and models for reference year climate data sets in Montreal for all time periods.

	EWY		TDY		ECY		
	Year	model	year	model	year	model	
2010s	Jan	2019	NCC	2012	MOHC	2007	MPI
	Feb	2011	NCC	2019	MOHC	2019	MPI
	Mar	2015	NCC	2008	MPI	2017	MPI
	Apr	2018	MPI	2007	MOHC	2002	MPI
	May	2008	MPI	2012	MPI	2019	NCC
	Jun	2014	MPI	2015	MOHC	2018	NCC
	Jul	2020	MPI	2015	MOHC	2003	NCC
	Aug	2020	MPI	2002	MOHC	2016	NCC
	Sep	2020	MOHC	2017	MOHC	2009	NCC
	Oct	2003	MOHC	2012	MPI	2011	MPI
	Nov	2020	NCC	2020	MOHC	2013	MPI
	Dec	2012	NCC	2007	MOHC	2013	MOHC
2050s	Jan	2044	NCC	2052	MOHC	2049	MPI
	Feb	2051	NCC	2042	MOHC	2058	MOHC
	Mar	2059	NCC	2056	MOHC	2058	MPI
	Apr	2044	MOHC	2043	MPI	2046	MPI
	May	2055	MOHC	2057	MPI	2046	NCC
	Jun	2054	MOHC	2059	MOHC	2050	NCC
	Jul	2051	MOHC	2043	MPI	2051	NCC
	Aug	2051	MOHC	2055	MPI	2049	NCC
	Sep	2051	MOHC	2055	MPI	2041	NCC
	Oct	2041	MOHC	2055	MOHC	2043	MPI
	Nov	2058	NCC	2052	MOHC	2056	MPI
	Dec	2056	NCC	2056	MOHC	2041	MPI
2090s	Jan	2088	NCC	2098	MOHC	2089	MPI
	Feb	2097	NCC	2098	MOHC	2096	MPI
	Mar	2088	NCC	2087	MOHC	2085	MPI
	Apr	2085	MOHC	2095	MOHC	2083	MPI
	May	2086	MOHC	2092	MOHC	2086	NCC
	Jun	2082	MOHC	2082	MPI	2087	NCC
	Jul	2082	MOHC	2085	MPI	2081	NCC
	Aug	2097	MOHC	2088	MPI	2088	NCC
	Sep	2082	MOHC	2088	MOHC	2099	MPI
	Oct	2087	MOHC	2099	MPI	2094	MPI
	Nov	2093	MOHC	2084	MOHC	2092	MPI
	Dec	2086	NCC	2096	MOHC	2090	MPI

temperature varies from -11.5°C to 19.8°C for Montreal, -3.7°C – 22.3°C for Toronto, and 3.6°C – 18°C for Vancouver. The daily maximum temperature varies from 12°C to 36.1°C for Montreal, 16.1°C – 40.6°C for Toronto, and 14.9°C – 34.4°C for Vancouver. The historical hottest month for three Canadian cities based on the average and maximum daily temperature is normally found in July or August. It

is clear that Toronto has the highest temperature during the summer periods, and Montreal tends to have the coldest winter. Compared with Montreal and Toronto, Vancouver is more likely to have a cool summer and slightly cold winter. Besides, Toronto and Montreal are climate locations where overheating is more likely to occur as compared to Vancouver, considering the historical daily maximum temperature for these locations. Average humidity varies from 73.2% to 90.4% for Montreal, 76.1%–89.6% for Toronto, and 81.3%–89.2% for Vancouver. It could be found that Montreal and Toronto have similar climate patterns where wet summers and dry winters are evident, whereas Vancouver has a different climate pattern from the other two eastern Canadian locations. Regarding the wind velocity, average wind speed varies from 7.2 m/s to 12.3 m/s for Montreal, 10 m/s to 14 m/s for Toronto, and 11.2 m/s to 13.2 m/s for Vancouver. Across the twelve months, the wind speeds are higher in winter in Montreal and Toronto, whereas the difference in monthly wind speeds in Vancouver is relatively small over the twelve months.

2.2. Climate models and observational data

The climate data to undertake simulations during the contemporary and future periods were collected from the Coordinated Regional Downscaling Experiment (CORDEX) database [74], which provides multi-modal regional climate simulations for many state-of-the-art regional climate models (RCMs) forced by different global climate models (GCMs) [75]. A review of data available in the CORDEX is conducted, and a total of three RCM-GCM combinations are found to have three hourly climate projections with all the climatic variables for building simulations available for the North American domain. These three GCM-RCM combinations are selected for this study. The GCMs associated with the selected projections are:

- (1) MPI-ESM-LR [76]: Climate projections based on the components of ECHAM6 for atmosphere and MPIOM for the ocean and JSBACH for the terrestrial biosphere, and HAMOCC for the ocean biogeochemistry.
- (2) NCC-NorESM1-M [77]: Climate projections of the first generation model developed by the Norwegian Climate Centre (NCC).
- (3) MOHC-HadGEM2-ES [78]: Climate projections of the second version of the Hadley Centre Global Environment Model (HadGEM2) by the Met Office Hadley Centre (MOHC).

The regional climate models associated with all three climate simulations were the hydrostatic version of the Regional Model [79] (version

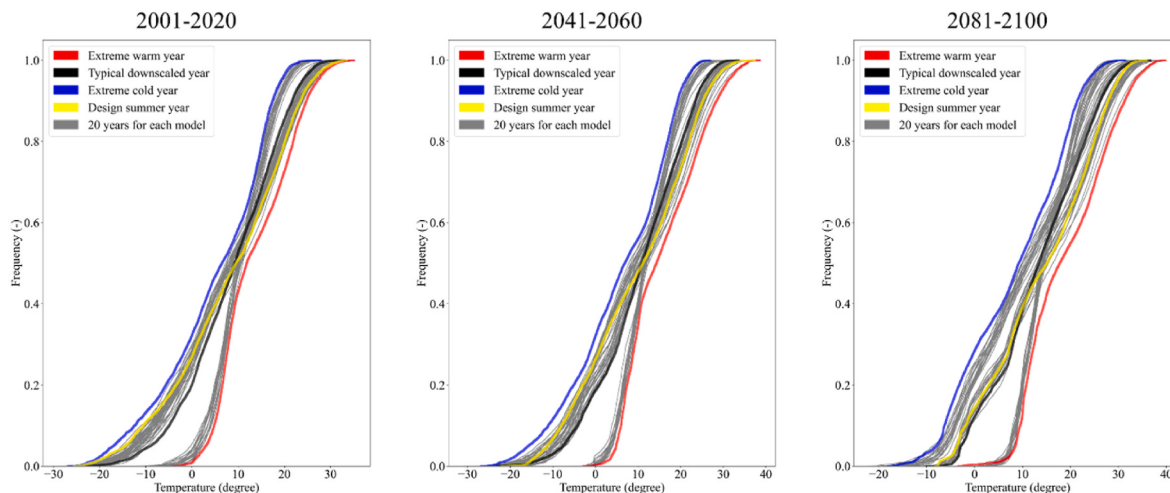
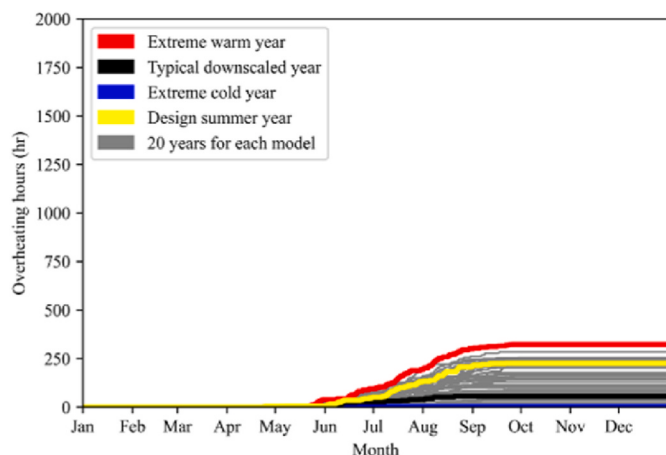
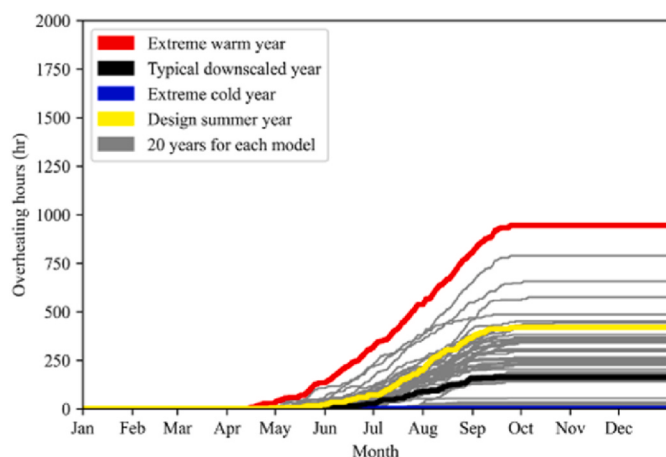


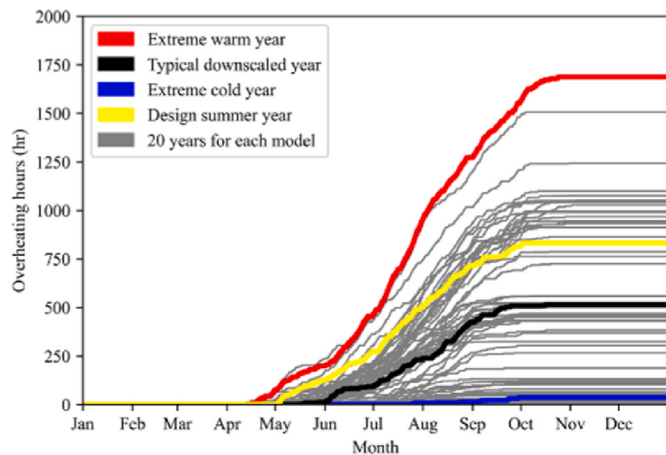
Fig. 4. Cumulative distribution function comparison of the hourly temperature from 20 years, DSY and 1-year reference year climate data sets of TDY, ECY, and EWY in Montreal for the contemporary term, mid-term and long-term future.



2001-2020



2041-2060



2081-2100

Fig. 5. The yearly outdoor overheating hours of TDY, EWY, ECY, DSY, and 20-year climate data for Montreal.

REMO 2015), which dynamically downscale the GCM projections to a horizontal resolution of 0.22° (25 km). The future projections as applied in this study correspond to RCP 8.5, which represents the high range of non-climate policy scenarios [80,81], assuming that by 2100, atmospheric concentrations of CO_2 will be three to four times higher than the pre-industrial levels. The global warming increases for RCP 8.5 are

Table 4

Outdoor overheating hours during the summer months in Montreal from TDY, ECY, EWY, entire 20-year data, and DSY.

Time periods	Model	May	June	July	August	September
2010s	ECY	0	1	0	0	0
	TDY	3	24	13	15	0
	EWY	36	56	99	107	22
	20-year (max.)	36	74	123	107	65
	20-year (avg.)	4	21	37	26	7
	20-year (min.)	0	0	0	0	0
	DSY	2	45	83	79	14
2050s	ECY	0	0	0	0	0
	TDY	2	23	63	68	7
	EWY	103	184	219	271	136
	20-year (max.)	103	184	219	271	136
	20-year (avg.)	10	34	74	78	26
	20-year (min.)	0	0	0	0	0
	DSY	16	51	129	169	51
2090s	ECY	0	0	8	5	23
	TDY	12	80	146	186	83
	EWY	123	264	494	316	290
	20-year (max.)	161	264	494	347	290
	20-year (avg.)	27	82	165	168	70
	20-year (min.)	0	0	3	0	0
	DSY	123	150	238	203	106

2.0 °C (around 1.4–2.6 °C) during mid-term future and 3.7 °C (around 2.6–4.8 °C) during long-term future [80]. For the selected GCM-RCM combinations, four climatic variables required for conducting building simulations were collected, including dry-bulb air temperature (tas), relative humidity (hurs), wind speed (sfcWind), and global solar radiation (rsds).

Besides, the observational data from local weather stations during the historical period are also collected. These observation data are downloaded from Canadian Weather Energy and Engineering Datasets (CWEEDS) [82] by Environment and Climate Change Canada from 1998 to 2017 for all three Canadian cities.

2.3. Bias correction of climate simulations

According to Maraun [83], the climate model bias is defined as ‘the systematic difference between a simulated climate statistic and the corresponding real-world climate statistics’. There are various reasons for the bias in climate model simulations, and the primary among them is the coarse resolution of climate models at which several local scale climate processes cannot be resolved [84–87]. Therefore, failure to eliminate the bias from climate model simulations can result in an inaccurate assessment of overheating in the cities over contemporary and future projected time periods.

Based on the literatures [83,85,88–90], it could be found that bias-correction is performed frequently when using climate model projections for local scale impact assessments and the bias associated with climate models are significantly reduced by the bias-correction step. Many bias-correction methods such as simple scaling and additive corrections [91–93], advanced histogram equalization [89,94,95], and multivariate methods [96,97] exist in the literature. In this study, climate projections are bias-corrected with the multivariate quantile mapping bias correction method: MBCn proposed by Cannon [96]. This method used an image processing technique which is N-dimensional probability density function transform, to transfer the observed continuous multivariate distribution to the corresponding multivariate distribution of variables from climate simulations [98,99].

2.4. Reference year selection

Owing to the existence of multiple GCMs and RCMs, considerable uncertainties exist in future climate projections [87]. To account for the

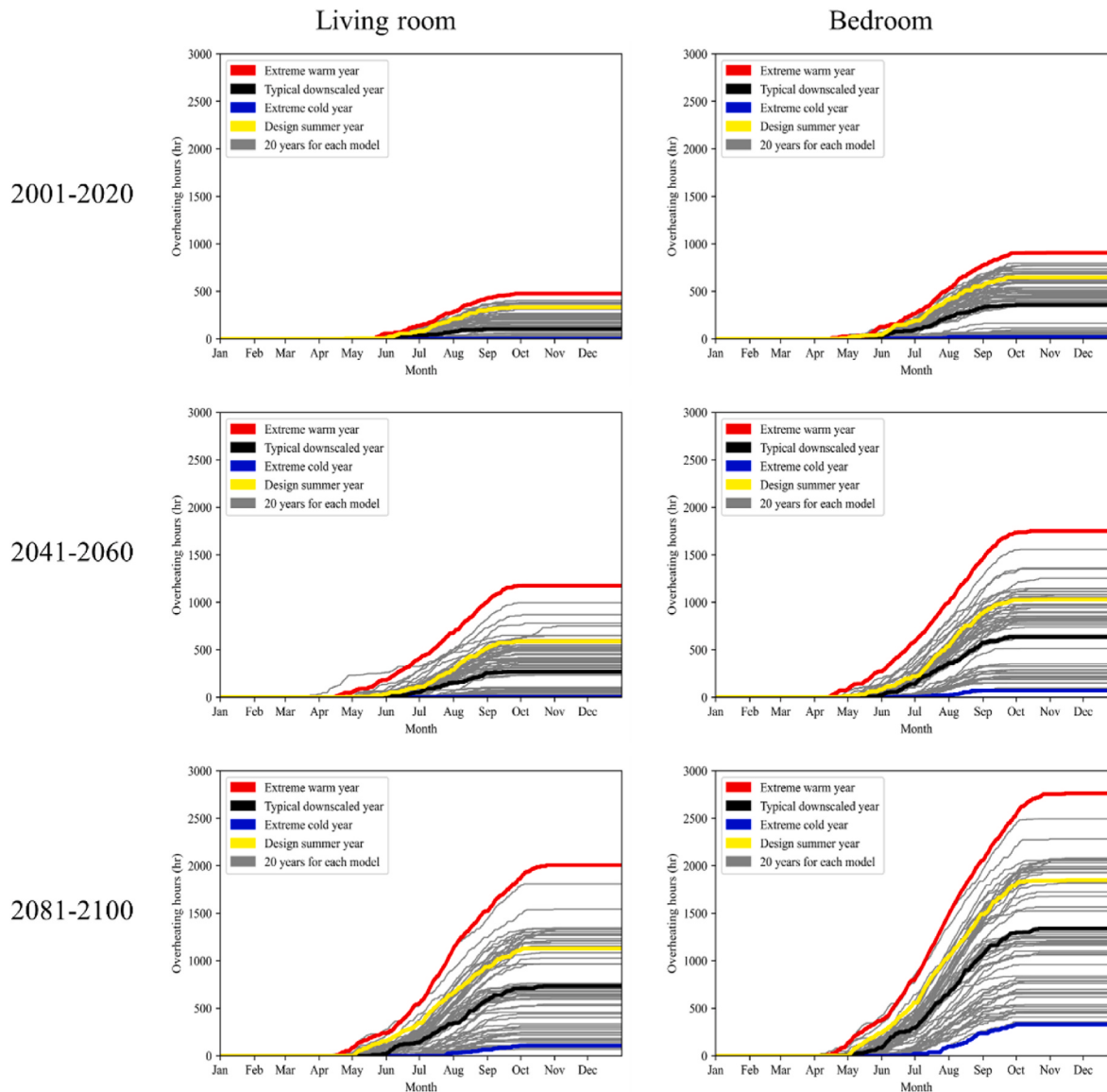


Fig. 6. Yearly cumulative indoor overheating hours in Montreal of reference year, DSY, and 20-years climate data.

uncertainties, ideally, the ensemble of climate projections needs to be considered when performing future overheating assessments. However, this is time-consuming and computationally expensive. Furthermore, climate change assessments are performed over multidecadal timescales, which makes the task of considering climate projections from multiple GCMs and RCMs even more challenging [100,101].

As discussed before, Nik [46] developed a method to select one typical and two extreme years of data to capture the range of climatic conditions present in an ensemble of future climate projections. Typical/extreme year data are prepared by identifying twelve typical/extreme meteorological months and combining them as one year of continuous data. For each month, the cumulative distribution function (CDF) of the outdoor air temperatures for each year is compared with the CDF of outdoor air temperatures from all years, and the year with the least absolute difference between them is identified as the typical month. Extreme cold and warm year data are prepared in a similar way. However, instead of selecting the month with the least absolute difference, the month with the maximum and minimum difference between CDFs is selected as the extremely warm and cold months, respectively. They are then combined to prepare the extremely cold year and extremely warm year data.

In this study, to evaluate the performance of the reference year data method, a Design Summer Year (DSY) by Levermore and Parkinson [62] is also prepared. The DSY was introduced in 2002 [102] by CIBSE to determine the warm weather data for assessing overheating risk in naturally ventilated and passively cooled buildings with dynamic simulation programs that represent a 'near extreme' warm weather [103]. The DSY is a selected one whole-year actual weather data from the multiple-year datasets within a given time period, normally around 20 years. The procedure to identify DSY first ranks the average dry bulb temperature from April to September of each year and then selects the year that falls in the top 12.5% quartile of the rank (i.e., the 3rd warmest year in a set of 20 years), assuming a uniform probability distribution as the DSY.

2.5. Building model and overheating criteria

An archetype building model of a typical single-detached Canadian home created by Laouadi et al. [45] is used in this study for the indoor simulation using EnergyPlus [104]. The home contains four thermal zones, which are the basement, first floor, second floor, and attic. Fig. 2 shows the geometry outline of this building. A uniform distribution of air

Table 5

Indoor overheating hours in the living room (liv) and bedroom (bed) during the summer months in Montreal from TDY, ECY, EWY, entire 20-year data, and DSY.

Time periods	Model	May		June		July		August		September	
		Liv	Bed	Liv	Bed	Liv	Bed	Liv	Bed	Liv	Bed
2010s	ECY	0	0	1	5	0	11	0	3	0	0
	TDY	9	26	28	69	35	129	30	107	0	27
	EWY	58	101	79	135	141	260	148	250	49	131
	20-year (max.)	58	102	101	180	158	265	148	250	91	153
	20-year (avg.)	7	22	33	76	59	138	47	117	13	39
	20-year (min.)	0	0	0	0	0	2	0	2	0	0
	DSY	5	34	73	150	127	222	96	149	27	84
2050s	ECY	0	0	0	0	2	7	0	10	0	0
	TDY	1	11	22	78	64	170	66	157	4	35
	EWY	95	161	181	267	218	351	285	410	130	223
	20-year (max.)	95	162	182	267	222	354	289	412	132	225
	20-year (avg.)	93	273	327	787	773	175	84	179	26	62
	20-year (min.)	0	0	0	0	0	6	0	10	0	0
	DSY	28	69	77	138	177	317	231	350	71	137
2090s	ECY	0	0	0	21	30	78	33	136	43	94
	TDY	19	76	122	208	202	366	242	408	127	231
	EWY	154	240	313	433	577	681	393	569	348	478
	20-year (max.)	195	289	313	433	577	681	414	605	348	485
	20-year (avg.)	373	717	1117	204	225	369	228	384	99	185
	20-year (min.)	0	0	0	11	17	79	29	137	0	10
	DSY	153	240	193	317	318	487	269	443	179	311

leakage over home surfaces is considered when windows are closed. The attic space has four intentional openings with a total area of 1/150 of the attic floor surface area for ventilation. The typical internal horizontal venetian blinds and exterior applied gray screen shades were applied with an openness factor of 5%. Windows are open by 25% when the indoor temperature is higher than the outdoor temperature and a set-point temperature of 24 °C. The window size for South and North is 2 m × 4 m, and the window size for East and West is 2 m × 2 m. Besides, there is no external obstructions around the building and no night cooling design. Some key information about the characteristics of the construction is shown in Table 2. For brevity, this paper does not include all the building details.

To evaluate the effects of extreme hot and cold climate conditions on the indoor temperature, the home is assumed to be free-running for the entire year. Detailed information about the characteristics of the construction is shown in Table. More details for all the building models can be found from the National Building Code of Canada (2015). The numbers of people for bedroom and living room are set as three and the fraction of room occupancy will change based on the schedule (Bedroom: 0.9 for 0:00–6:00, 0 for 6:00–21:00, 0.9 for 21:00–24:00; Living room: 0 for 0:00–6:00, 0.7 for 6:00–7:00, 0.4 for 7:00–8:00, 0.3 for 8:00–16:00, 0.5 for 16:00–17:00, 0.9 for 17:00–21:00, 0 for 21:00–24:00). The solar radiation data for building simulation include three components, which are global solar radiation obtained from CORDEX database and bias-corrected using MBCn method, and direct normal and diffuse solar radiation calculated from the bias-corrected global radiation [105].

Evaluating overheating risks of buildings requires the determination of appropriate overheating criteria [5]. The PMV/PPD thermal comfort model [107] (PMV stands for predicted mean vote and PPD stands for predicted percentage dissatisfied) developed by Fanger is widely applied to the overheating assessment by various standards such as EN [108], ISO [109], ASHARE [110], and CIBSE [111], suggesting different PMV/PPD static comfort limits under different building operation types. Due to the difficulty of measuring PMV in various indoor environments, some standard translate the PMV/PPD ranges into the operative temperature scales. In CIBSE TM52 [112], the PMV/PPD ranges is translated by assuming specific relative humidity (=50%), air velocity (<0.1 m/s), metabolic rate (1.2 met), and clothing factor (0.5 clo for summer). Accordingly, the temperature thresholds of the residential building are determined as 26 °C and 28 °C for the living room and bedroom,

respectively. With the thresholds temperature, the overheating risks could then be evaluated by the hours of exceedance [112], indoor overheating degree [3], and heat exposure index [113]. Besides, Robinson and Haldi [114,115] also developed a mathematical model for predicting overheating risk under various environmental conditions, considering the analogy between the charging and discharging of human's tolerance to overheating stimuli. Comparing with the data from the field survey, the application of this analytical model provided encouraging results.

In this work, a fixed temperature threshold value was used for the overheating assessment. For the indoor scenario, the overheating baseline temperatures are chosen as 28 °C for the living room and 26 °C for the bedroom following previous studies [111,112,116]. For the outdoor scenario, the threshold value is selected as 28 °C based on the previous work by Chang et al. [19]. The overheating hours were defined as the number of hours when the air temperature difference between the baseline and simulated temperature is greater than or equal to one degree following the concept of hours of exceedance from the guideline of CIBSE TM52 [112]:

$$h_{outOH} = \sum h_{Tout-28 \geq 1} \quad (1)$$

$$h_{livOH} = \sum h_{Tliv-28 \geq 1} \quad (2)$$

$$h_{bedOH} = \sum h_{Tbed-28 \geq 1} \quad (3)$$

where, h_{outOH} is the outdoor overheating hours, h_{livOH} is the indoor overheating hour for the living room, h_{bedOH} is the indoor overheating hour for the bedroom, $h_{Tout-28 \geq 1}$ is the hour of exceedance for the outdoor scenario, $h_{Tliv-28 \geq 1}$ is the hour of exceedance for living room, and $h_{Tbed-28 \geq 1}$ is the hours of exceedance for bedroom.

3. Results and discussion

3.1. Bias correction of climate simulations

The cumulative distribution function (CDF) of observations (gray curve), raw RCM data (blue curve), and RCM data bias-corrected using MBCn method (red curve) is shown in Fig. 3. The results for the other two driving models, and their results share the same pattern as given in Fig. 3, so they are not included here for the sake of brevity. The

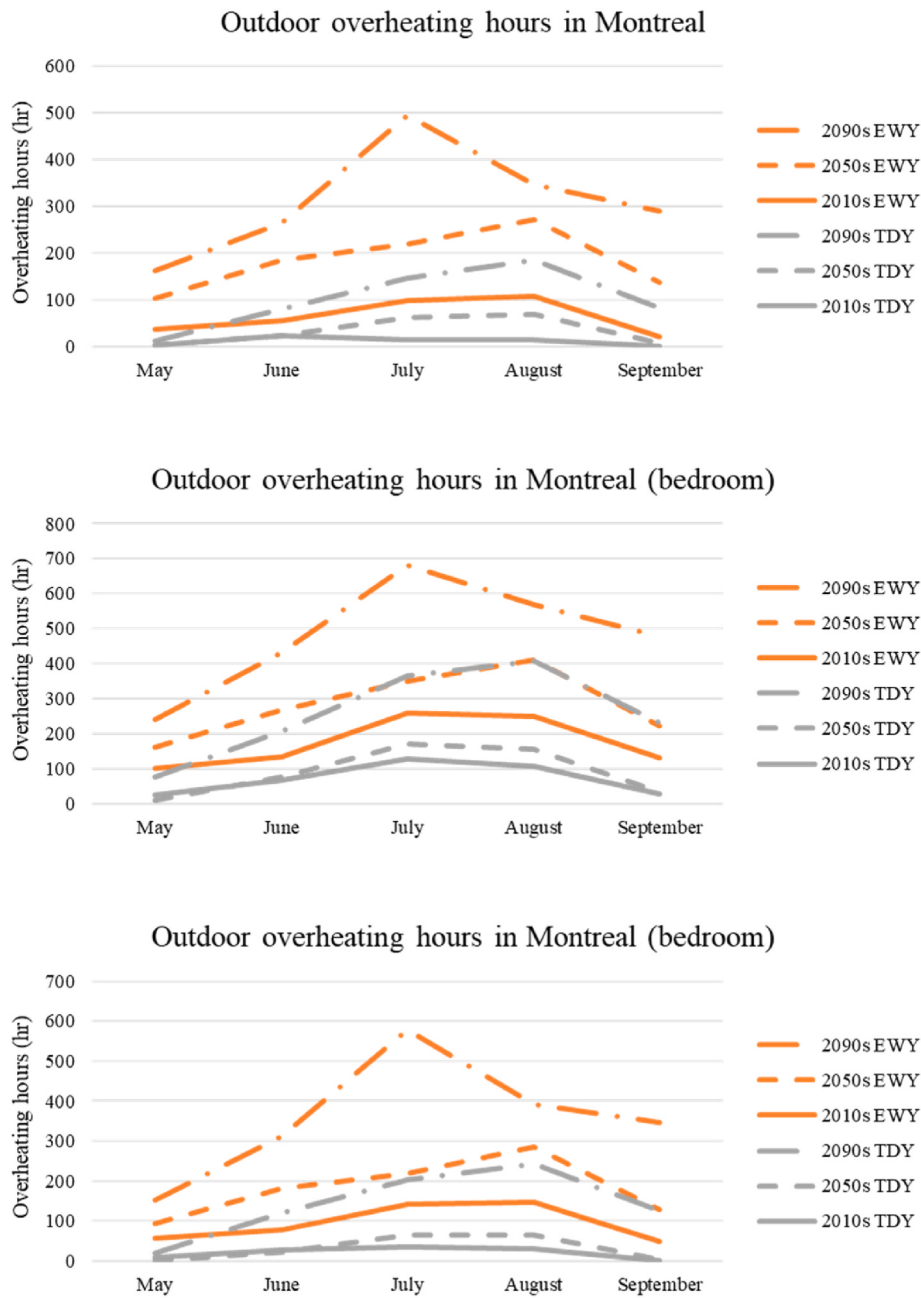


Fig. 7. Outdoor and indoor overheating hours of EWY and TDY for Montreal among three time periods.

comparison of CDFs for Toronto and Vancouver can be found in Appendix A.1. It is clear that the bias-corrected climate data shares a similar pattern to the observational data.

Here, by using the historical weather data, the importance of conducting bias correction of the projected/estimated weather data could be shown. Without the bias correction, the average errors between observational data and RCM data for Montreal are 2.78 °C for air temperature, 68.3 W/m² for global solar radiation, 0.9 m/s for wind speed, and 14.5% for relative humidity. With the bias correction, these errors respectively decrease to: 0.05 °C, 0.1 W/m², 0.001 m/s and 0.01%. The MBCn bias correction method calibrated over the observational time-period is used to correct RCM data in the future time periods. By applying this bias correction method, the reliability of future bias-corrected RCM data will be increased and therefore, for any future weather projection study, bias correction is one of the most important steps.

3.2. Assessment of selected reference years in an overheating context

As has been illustrated in Section 2.4, the bias-corrected climate data generated were used to obtain reference year climate data. Here, an example case for Montreal is given, whose data were collected from the contemporary climate data set term, using three driving models (MPI, NCC, MOHC). Then, the reference years (TDY, EWY, ECY) were generated by combining the reference calendar months from the selected year and the designated driving model as shown in Table 3. In Fig. 4, a comparison is given of the distribution of outdoor temperature between the original 20-years and reference year data sets from three driving models. The reference year climate data sets are single-year data as shown by the blue curve (extreme cold year), black curve (typical down-scaled year), and red curve (extreme warm year). The yellow curve represents the temperature distribution of the DSY for the same time period. It is obvious that the temperature distribution of TDY is similar

to that of the general distribution for the 20-year data set for all three driving models which means TDY can represent the general temperature distribution of 20-year data. Besides, the distribution of ECY and EWY provides the upper and lower boundary for the 20-year data set. Therefore, the reference year datasets could be used to represent both the general trend of multiple years temperature distribution as well as its upper and lower temperature limit.

A similar trend could also be found for the other time periods and the other Canadian cities. The temperature distribution for DSY is more similar to that of the TDY that might be because DSY is generated as the third-warmest year. Compared with DSY, the EWY would likely capture a relatively extreme hot climate with the same temperature database. On the contrary, ECY would represent a relatively extreme cold climate. More detailed information of the nonparametric comparison for three Canadian cities over the three time periods investigated in this study can be found in [Appendix A.2](#).

The validation of the selected reference years is performed by comparing monthly outdoor and indoor overheating hours over the summer season from: 1) the data from the entire 20-years; 2) data from the three reference years: TDY, ECY, EWY; and 3) data from DSY. The cumulative yearly outdoor overheating hours of TDY (black line), EWY (red line), ECY (blue line), DSY (yellow line), and 20-year climate data (gray lines) for Montreal is presented in [Fig. 5](#) while the results for Toronto and Vancouver are presented in [Appendix B.1](#). It can be seen that the ECY and EWY are able to encompass the range of yearly overheating values simulated in the entire 20-year climate data. This is consistently observed for both contemporary and future time-periods, and the three cities.

[Table 4](#) presents outdoor overheating hours during the summer months from the reference years: TDY, ECY, EWY, DSY along with the maximum (max.), minimum (min.), and average (avg.) yearly 20-year values. The results for Toronto and Vancouver can be found in [Appendix B.2](#). In general, the maximum overheating values over the 20-years are close to the values of EWY for all cities and time-periods. The maximum outdoor overheating hours found in 20-years data of three Canadian cities considering both contemporary and future time-periods is 532 h (Toronto, July 2081–2100) which is same as the maximum outdoor overheating hours found in the synthesizing data (EWY, Toronto, July 2081–2100).

The average differences in overheating hours between TDY and average yearly 20-year values are 32.61% for Montreal, 1.89% for Toronto, and 47.31% for Vancouver. The average differences in overheating hours between EWY and maximum yearly 20-year values are 9.5% for Montreal, 8.83% for Toronto, and 22.51% for Vancouver. The average differences in overheating hours between ECY and min. yearly 20-year values are relatively small, generally less than 10 h. On the other hand, the differences between DSY and max. yearly 20-year values are larger than 20% in most cases, and in some cases even larger than 60%.

Above results suggest that TDY, EWY and ECY could efficiently capture average, maximum and minimum monthly outdoor overheating conditions simulated in the entire 20-year data. The EWY and ECY are able to provide upper and lower boundaries of possible outdoor overheating conditions in the cities. The EWY is able to better capture outdoor overheating conditions than the DSY and hence is more suitable to represent extreme overheating conditions in the cities.

To assess the efficacy of the reference year selection method in indoor overheating context, this study firstly simulated the indoor temperature in a free-running single house building model and compared indoor overheating from the entire 20-years climate data with the TDY, EWY, ECY, and DSY reference years. [Fig. 6](#) reports the yearly cumulative indoor overheating hours for Montreal whereas the results for Toronto and Vancouver can be found in [Appendix B.3](#). The results for basement and attic are not presented in this paper as these areas are typically not frequently occupied by the home occupants as compared to other areas.

[Table 5](#) presents indoor overheating hours in the living room (liv) and bedroom (bed) during the summer months from the reference years:

TDY, ECY, EWY, DSY along with the maximum, minimum, and average yearly 20-year values. The results for Toronto and Vancouver can be found in [Appendix B.4](#). The average difference between TDY and avg. yearly 20-year values is -18.42% for Montreal, -1.01% for Toronto, and 27.66% for Vancouver. The average difference in percentage between EWY and Max is 5.98% for Montreal, 2.82% for Toronto, and -9.05% for Vancouver. On the other hand, the average difference between DSY and Max is -37.92% for Montreal, -37.42% for Toronto, and -63.73% for Vancouver.

It can be deduced from the above results that EWY and ECY are able to efficiently capture upper and lower bounds of indoor overheating hours effectively. The EWY is able to represent the upper end of the overheating spectrum more effectively than DSY. A similar conclusion could be achieved for TDY that the average difference in yearly indoor overheating hours between TDY and Ave for three Canadian cities is relatively low, only around 0.9%.

3.3. Use of reference years to assess future projected changes in overheating

In this section, both outdoor and indoor overheating hours of TDY and EWY of mid-term and long-term future are compared with those of contemporary term to evaluate the impacts of climate change on future overheating in the cities. [Fig. 7](#) shows an example of changes in both outdoor and indoor overheating hours for Montreal among three different time periods. A similar trend is also found in Toronto and Vancouver, but due to the limit of paper, the graphical results are not reported.

Due to the impacts of climate change, a similar increase trend could be found in overheating hours in the three Canadian cities according to the results shown in [Tables 4 and 5](#); average monthly overheating hours increase by normally around one time (from 50% to 150%) until the mid-term future and by normally around two to three times (even up to 8 times for some scenarios) during the long-term future. For instance, the most obvious increase in outdoor overheating hours among two future terms is found in Montreal; the overheating hours of TDY increase by two times by mid-term future and by nine times for long-term future and that of EWY increase by two times and three and a half times by mid-term and long-term future. In opposite, the increase in both indoor and outdoor overheating hours for Vancouver is relatively small, and only around half time by mid-term future and one time by long-term future. It could also be clearly found in [Appendix B.1 and B.3](#) that it is more likely to find extra indoor and outdoor overheating hours appearing in the months not in the defined summer period (such as April and October) for the mid-term and long-term future.

4. Conclusion

This paper evaluates outdoor extreme heat events and indoor overheating conditions for a representative residential building located in three Canadian cities (Montreal, Toronto, and Vancouver) over contemporary (2001–2020), near-term future (2041–2060), and long-term future (2081–2100) time periods. The regional climate simulations forced by three GCMs were bias-corrected with reference to historical observations recorded at the airport location of the cities. Regard that although the analysis is performed for airport locations which may not be representative of fully developed urban areas, the methodology used is generalized enough to be used in urban locations.

Thereafter, a reference year selection method is used to generate three representative climate data years: typical downscaling year (TDY), extreme cold year (ECY), and extreme warm year (EWY).

The performance of TDY, ECY, and EWY climate data sets in capturing the range of overheating conditions present in the entire 20-year long contemporary and future projected time-periods is assessed. At the same time, the projected changes from the selected reference years and 20-year datasets are compared. The results are also compared

with a widely used metric of overheating: the design summer year (DSY). Based on the results, given in Sections 3.1, 3.2, and 3.3, following deductions from the study were obtained:

- (1) The multivariate quantile mapping bias correction method is able to improve the reliability of future climate data by capturing the distribution pattern of climatic variables as well as reducing errors and therefore, for any future weather projection study, bias correction is one of the most important steps.
- (2) For both outdoor/indoor overheating evaluation, EWY and ECY could efficiently capture maximum and minimum monthly overheating hours providing the upper and lower boundary of possible outdoor and indoor overheating conditions. TDY could be used to simulate the typical yearly overheating condition. The EWY captures the extreme overheating conditions better than the DSY.
- (3) Owing to the effects of climate change, a similar increase could be found in both indoor and outdoor overheating hours in the three Canadian cities; average monthly overheating hours increase by normally around one time (from 50% to 150%) until the mid-term future and by normally around two to three times (even up to nine times for some scenarios) during the long-term future.

As concluded in this study, it is recommended to use an accurate and time-saving method (reference year data set) to evaluate the future outdoor and indoor overheating conditions by generating the representative year climate data as the typical and extreme scenarios. The limitations of the current work are:

- (1) Only considering three Canadian cities for analysis;
- (2) Only the projections from three GCMs and one RCP scenario (RCP 8.5) was considered for preparing the climate data sets;
- (3) Only testing this method with the single-house building and assuming the features of the single-house building stay constant in all future years. In reality, the features of existing buildings will change based on age.

- (4) Only applying a fixed temperature threshold as the indoor and outdoor overheating criteria.

Future work will be directed to address some of the above limitations. Nevertheless, the study provides important results to support the use of reference year selection method described in Nik [44] for overheating assessments in cities around the globe.

CRediT authorship contribution statement

Jiwei Zou: Writing – review & editing, Writing – original draft, Visualization, Validation, Software, Methodology, Investigation, Formal analysis, Data curation, Conceptualization. **Abhishek Gaur:** Writing – review & editing, Supervision, Resources, Project administration. **Liangzhu (Leon) Wang:** Writing – review & editing, Supervision, Project administration, Funding acquisition. **Abdelaziz Laouadi:** Writing – review & editing. **Michael Lacasse:** Writing – review & editing.

Declaration of competing interest

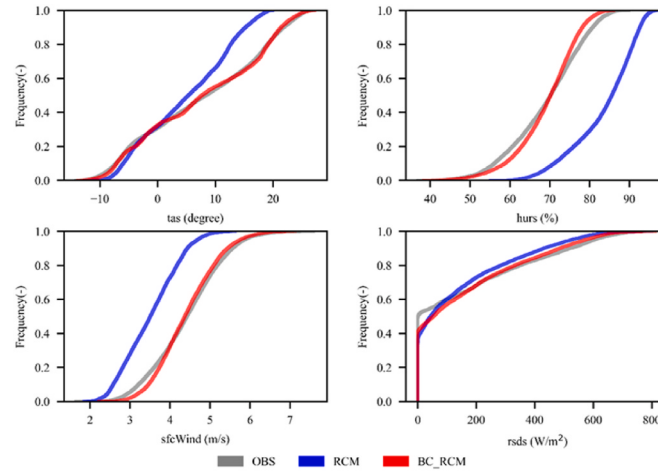
The authors declare that they have no known competing financial interests or personal relationships that could have appeared to influence the work reported in this paper.

Acknowledgment

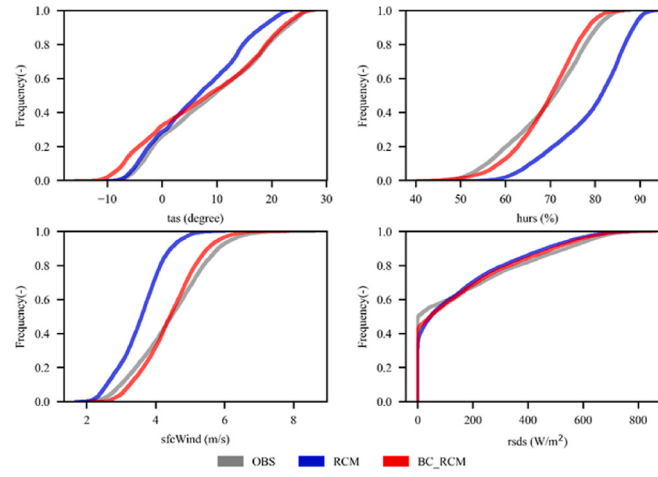
This work was supported by the Natural Sciences and Engineering Research Council of Canada (NSERC) through the Discovery Grants Program [#RGPIN-2018-06734] and the Advancing Climate Change Science in Canada Program [#ACCPJ 535986-18], and the Construction Research Centre of the National Research Council of Canada through funding from Infrastructure Canada in support of the Pan Canadian Framework on Clean Growth and Climate Change. The authors were very thankful for their supports.

Appendix A

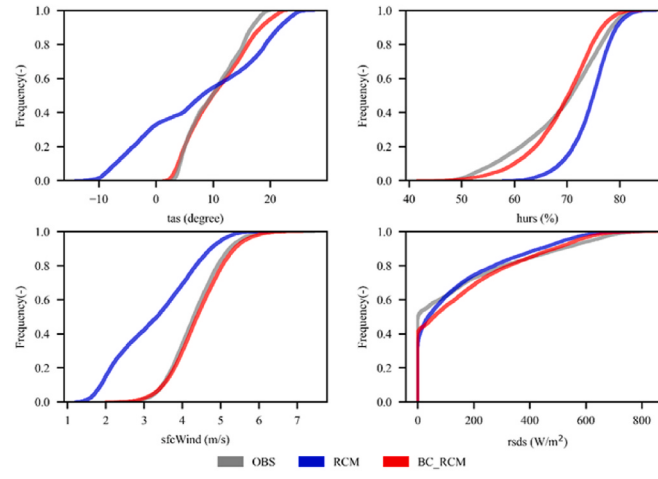
A.1. Cumulative distribution function comparison of observational (gray curve), raw RCM (blue curve) and bias-corrected RCM data (red curve) of sfcWind, tas, rsds, hurs (MPI, 1998–2017)



(a) Montreal

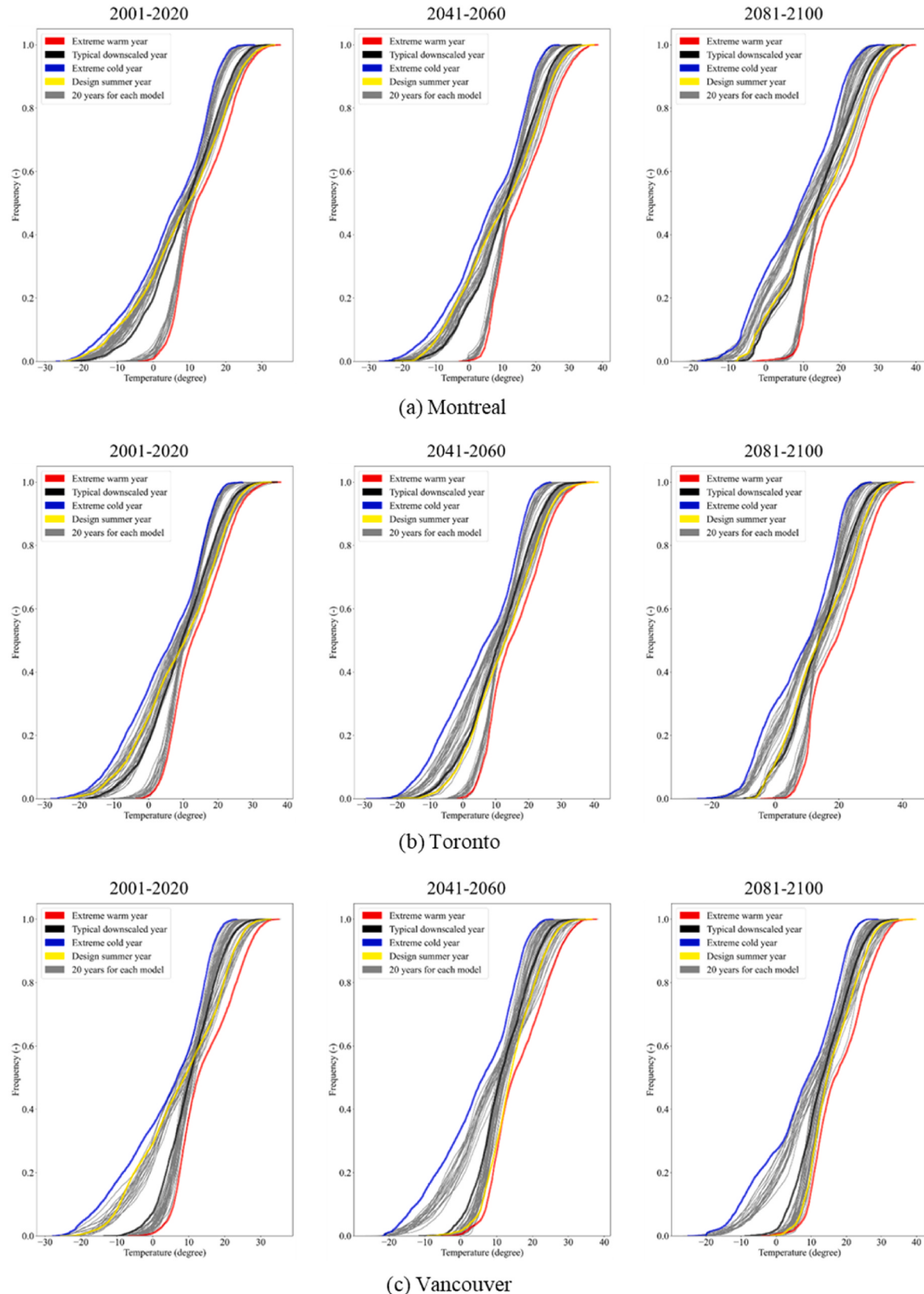


(b) Toronto



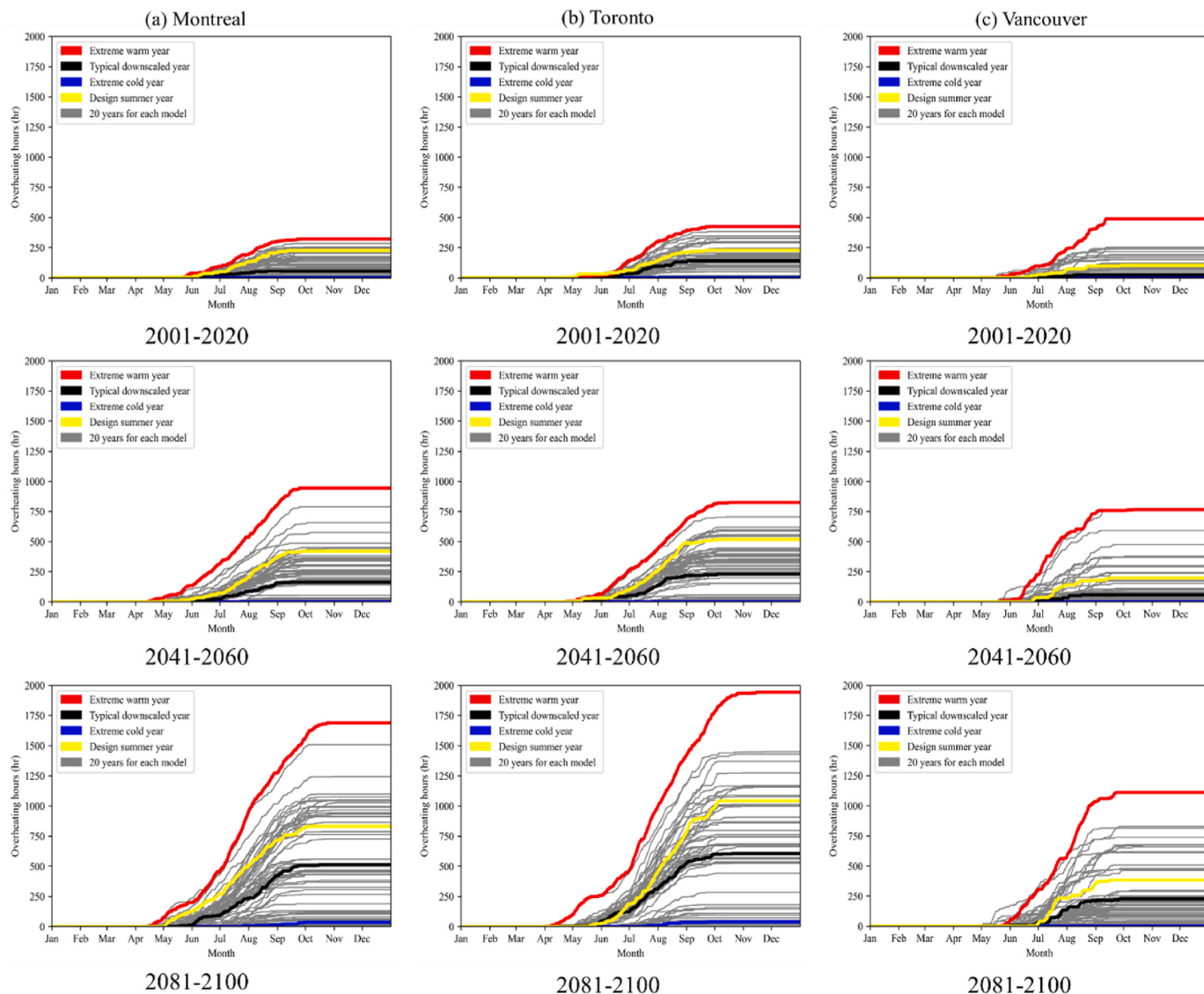
(c) Vancouver

A.2. Cumulative distribution function comparison of the hourly temperature from 20 years and reference year climate data sets of TDY, ECY and EWY



Appendix B

B.1. Yearly cumulative outdoor overheating hours in three Canadian cities



B.2. Monthly outdoor overheating hours between reference year and 20-years data sets in three Canadian cities

(a) Montreal

Time periods	Model	May	June	July	August	September
2010s	ECY	0	1	0	0	0
	TDY	3	24	13	15	0
	EWY	36	56	99	107	22
	20-year (max.)	36	74	123	107	65
	20-year (avg.)	4	21	37	26	7
	20-year (min.)	0	0	0	0	0
2050s	DSY	2	45	83	79	14
	ECY	0	0	0	0	0
	TDY	2	23	63	68	7
	EWY	103	184	219	271	136
	20-year (max.)	103	184	219	271	136
	20-year (avg.)	10	34	74	78	26
	20-year (min.)	0	0	0	0	0

(continued on next page)

(continued)

Time periods	Model	May	June	July	August	September
2090s	DSY	16	51	129	169	51
	ECY	0	0	8	5	23
	TDY	12	80	146	186	83
	EWY	123	264	494	316	290
	20-year (max.)	161	264	494	347	290
	20-year (avg.)	27	82	165	168	70
	20-year (min.)	0	0	3	0	0
	DSY	123	150	238	203	106

(b) Toronto

Time periods	Model	May	June	July	August	September
2010s	ECY	0	0	0	0	0
	TDY	8	27	62	34	9
	EWY	21	120	154	96	31
	20-year (max.)	39	120	165	108	56
	20-year (avg.)	4	27	46	30	11
	20-year (min.)	0	0	0	0	0
	DSY	29	30	80	69	18
2050s	ECY	0	0	0	0	0
	TDY	14	39	82	83	6
	EWY	63	195	181	243	129
	20-year (max.)	69	195	206	243	133
	20-year (avg.)	12	41	93	89	30
	20-year (min.)	0	0	0	0	0
	DSY	30	72	157	227	25
2090s	ECY	0	0	9	27	3
	TDY	42	78	191	214	72
	EWY	159	208	532	429	356
	20-year (max.)	159	208	532	429	356
	20-year (avg.)	35	83	196	189	75
	20-year (min.)	0	0	5	2	0
	DSY	26	162	269	335	198

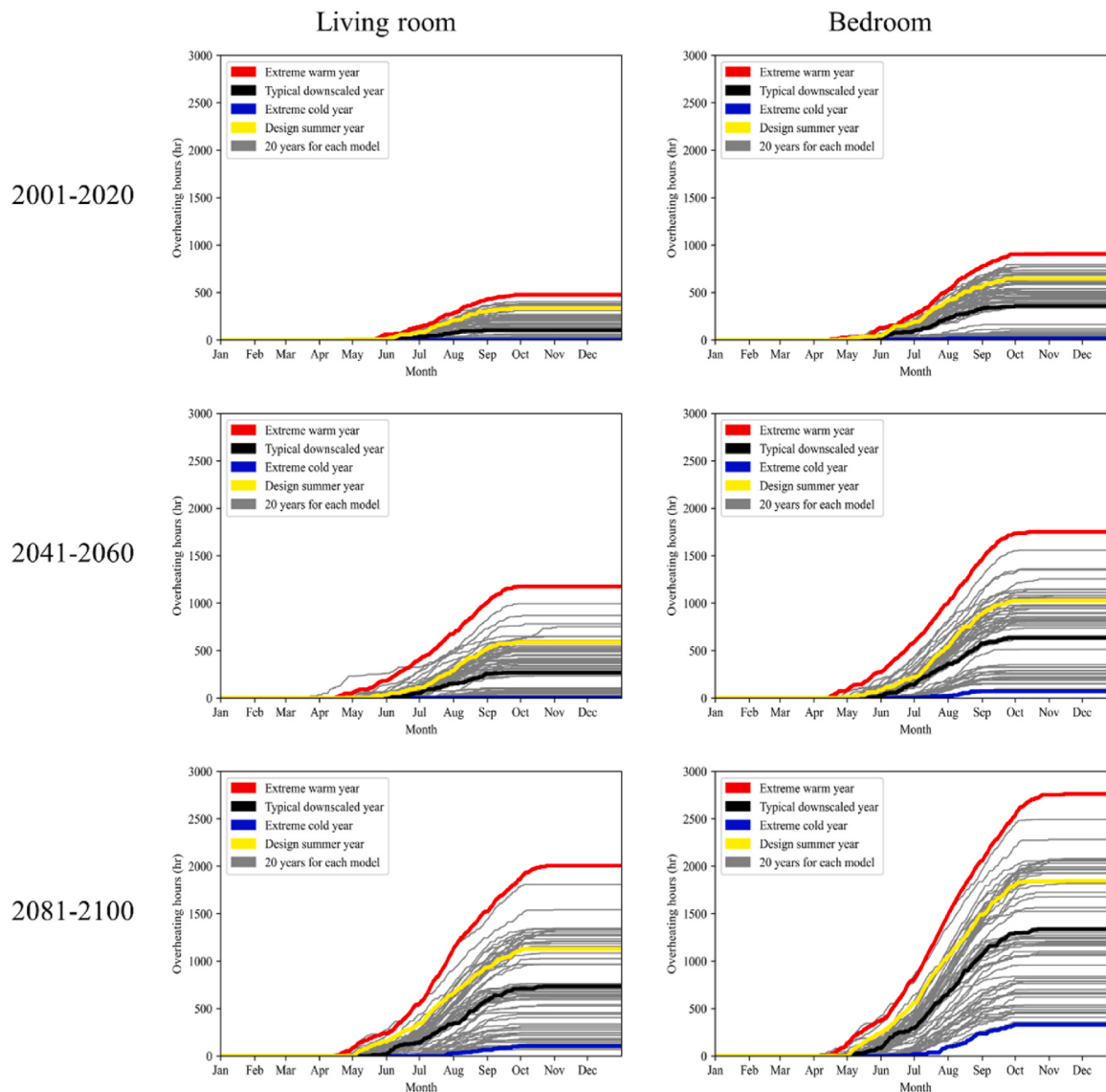
(c) Vancouver

Time periods	Model	May	June	July	August	September
2010s	ECY	0	0	0	0	0
	TDY	0	6	10	8	0
	EWY	27	69	145	162	84
	20-year (max.)	50	78	145	162	84
	20-year (avg.)	2	10	20	12	4
	20-year (min.)	0	0	0	0	0
	DSY	0	26	44	28	3
2050s	ECY	0	0	0	0	0
	TDY	0	11	22	23	0
	EWY	11	217	332	176	23
	20-year (max.)	102	217	341	191	73
	20-year (avg.)	4	21	39	31	9
	20-year (min.)	0	0	0	0	0
	DSY	0	33	108	37	21
2090s	ECY	1	0	0	0	0
	TDY	7	26	102	76	17
	EWY	49	250	278	459	75
	20-year (max.)	162	246	295	435	133
	20-year (avg.)	10	31	88	74	24
	20-year (min.)	0	0	0	0	0
	DSY	9	22	210	122	29

B.3. Yearly cumulative indoor overheating hours in three Canadian cities

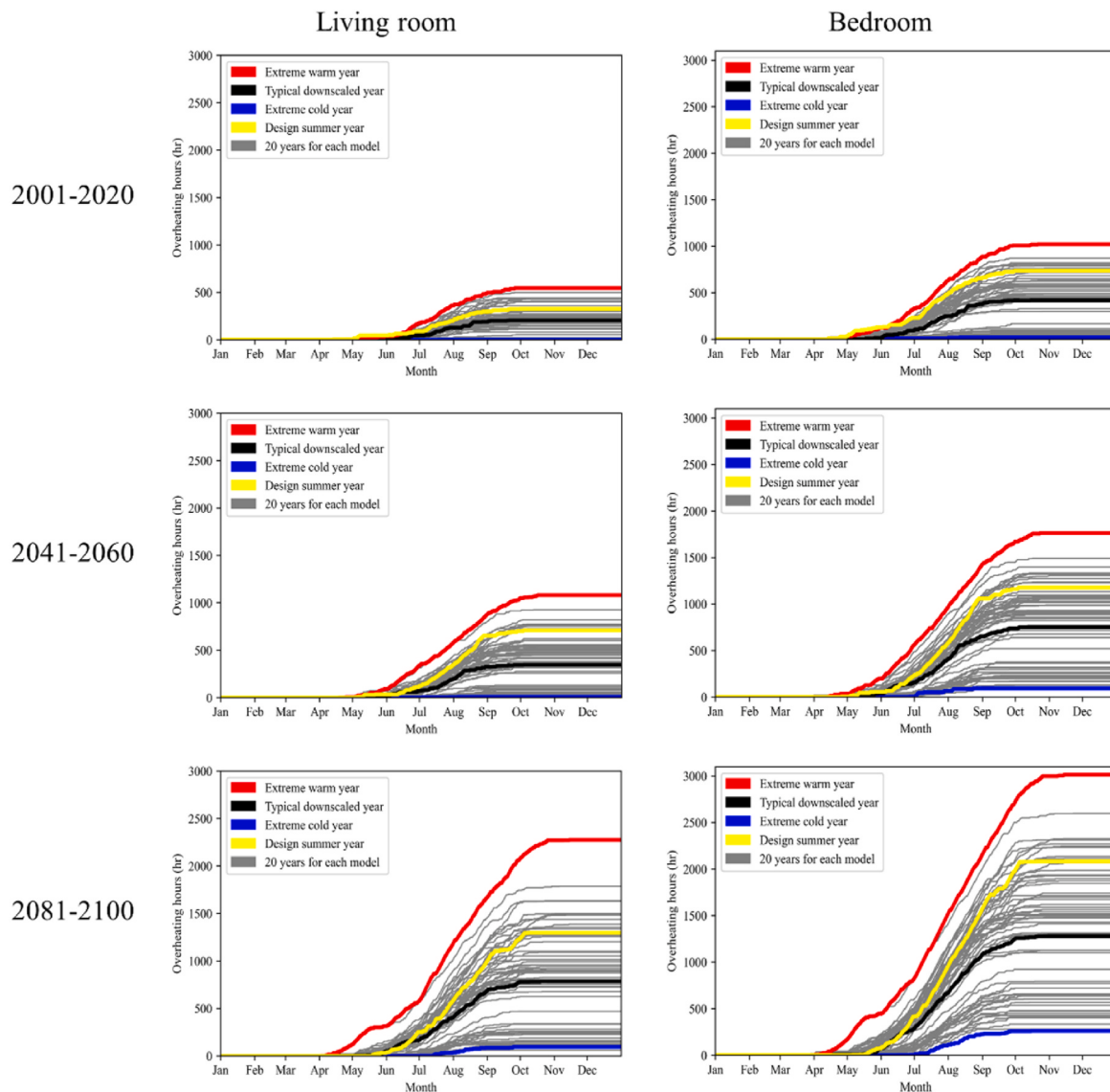
(a) Montreal

(a) Montreal



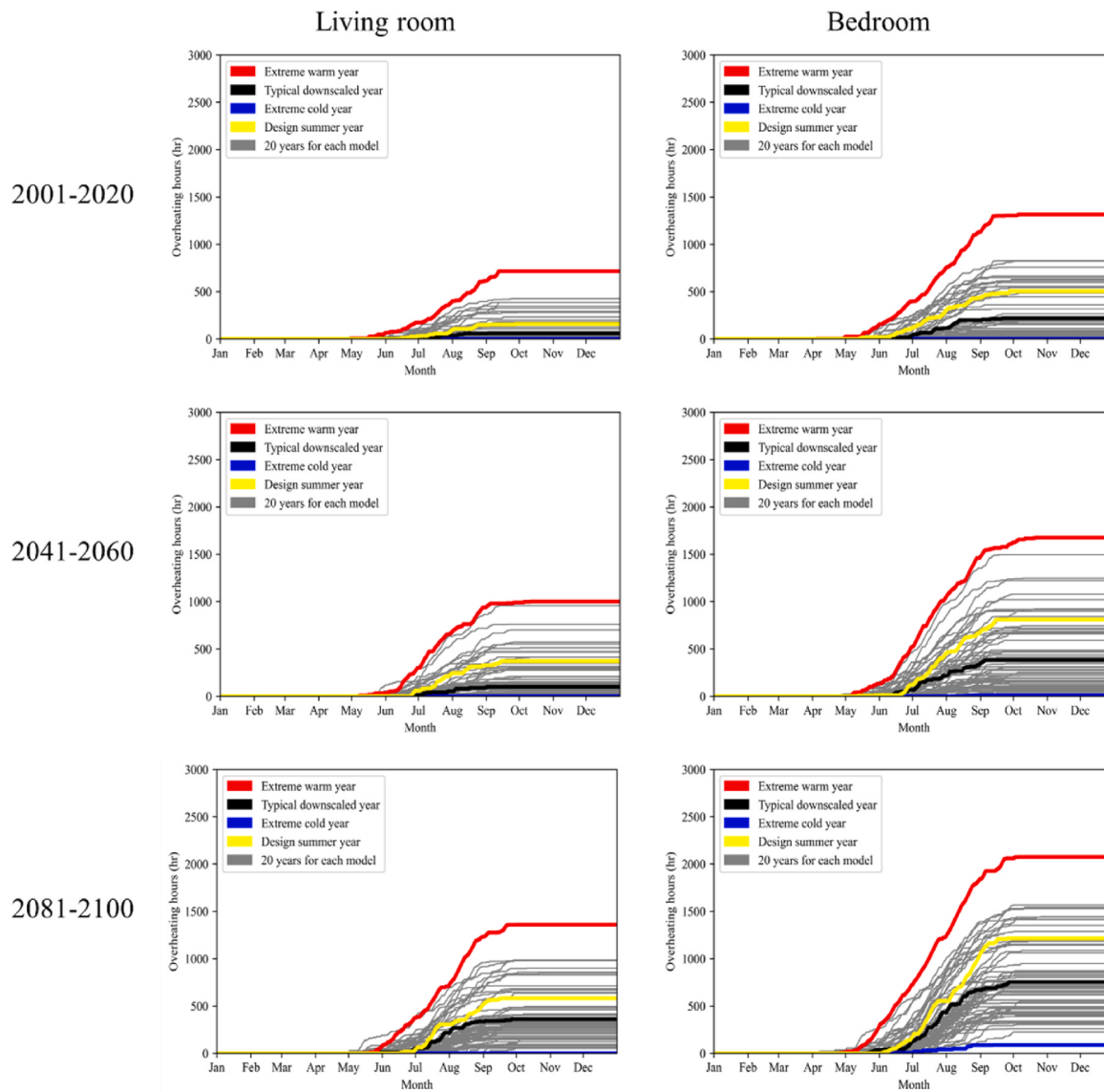
(b) Toronto

(b) Toronto



(c) Vancouver

(c) Vancouver

**B.4. Difference in monthly indoor overheating hours between synthesizing and 20-years data sets in three Canadian cities (Liv: Living room, Bed: Bedroom)**

(a) Montreal

Time periods	Model	May		June		July		August		September	
		Liv	Bed	Liv	Bed	Liv	Bed	Liv	Bed	Liv	Bed
2010s	ECY	0	0	1	5	0	11	0	3	0	0
	TDY	9	26	28	69	35	129	30	107	0	27
	EWY	58	101	79	135	141	260	148	250	49	131
	20-year (max.)	58	102	101	180	158	265	148	250	91	153
	20-year (avg.)	7	22	33	76	59	138	47	117	13	39
	20-year (min.)	0	0	0	0	0	2	0	2	0	0
	DSY	5	34	73	150	127	222	96	149	27	84
2050s	ECY	0	0	0	0	2	7	0	10	0	0
	TDY	1	11	22	78	64	170	66	157	4	35
	EWY	95	161	181	267	218	351	285	410	130	223
	20-year (max.)	95	162	182	267	222	354	289	412	132	225
	20-year (avg.)	93	273	327	787	773	175	84	179	26	62

(continued on next page)

(continued)

Time periods	Model	May		June		July		August		September	
		Liv	Bed	Liv	Bed	Liv	Bed	Liv	Bed	Liv	Bed
2090s	20-year (min.)	0	0	0	0	0	6	0	10	0	0
	DSY	28	69	77	138	177	317	231	350	71	137
	ECY	0	0	0	21	30	78	33	136	43	94
	TDY	19	76	122	208	202	366	242	408	127	231
	EWY	154	240	313	433	577	681	393	569	348	478
	20-year (max.)	195	289	313	433	577	681	414	605	348	485
	20-year (avg.)	373	717	1117	204	225	369	228	384	99	185
	20-year (min.)	0	0	0	11	17	79	29	137	0	10
	DSY	153	240	193	317	318	487	269	443	179	311

(b) Toronto

Time periods	Model	May		June		July		August		September	
		Liv	Bed	Liv	Bed	Liv	Bed	Liv	Bed	Liv	Bed
2010s	ECY	0	11	0	0	0	4	0	6	0	0
	TDY	9	14	36	82	85	151	60	131	16	40
	EWY	31	88	141	208	183	303	135	256	48	119
	20-year (max.)	45	93	141	208	194	316	155	293	73	137
	20-year (avg.)	6	20	37	81	66	144	49	116	17	46
	20-year (min.)	0	0	0	0	0	4	0	6	0	0
	DSY	41	94	43	102	118	261	89	168	29	77
	ECY	0	0	0	5	6	62	2	26	0	0
2050s	TDY	19	41	53	118	128	255	125	240	20	83
	EWY	84	165	249	360	245	408	299	459	166	243
	20-year (max.)	94	172	249	360	269	410	299	470	166	243
	20-year (avg.)	16	39	55	114	136	261	128	243	43	88
	20-year (min.)	0	0	0	0	0	41	1	26	0	0
	DSY	34	53	90	178	224	350	307	473	47	104
	ECY	0	0	0	3	35	110	50	114	9	33
	TDY	48	72	113	207	240	383	283	416	93	167
2090s	EWY	194	277	266	378	605	697	487	633	411	568
	20-year (max.)	194	277	267	390	596	698	503	650	411	568
	20-year (avg.)	45	85	115	209	255	402	253	405	101	188
	20-year (min.)	0	0	0	3	27	110	29	114	0	2
	DSY	35	80	217	336	334	542	413	614	240	415

(c) Vancouver

Time periods	Model	May		June		July		August		September	
		Liv	Bed	Liv	Bed	Liv	Bed	Liv	Bed	Liv	Bed
2010s	ECY	0	0	0	0	0	0	0	0	0	0
	TDY	0	0	9	29	27	73	22	87	1	20
	EWY	57	133	108	242	227	360	214	375	102	171
	20-year (max.)	64	133	108	242	227	360	214	376	102	171
	20-year (avg.)	3	10	15	39	35	89	25	72	6	20
	20-year (min.)	0	0	0	0	0	0	0	0	0	0
	DSY	0	20	31	102	65	185	54	130	8	68
	ECY	0	0	0	0	0	0	0	8	0	2
2050s	TDY	0	10	12	57	41	149	42	129	4	37
	EWY	35	132	266	394	384	527	259	421	46	150
	20-year (max.)	119	150	264	396	397	546	256	417	97	193
	20-year (avg.)	7	19	30	64	64	149	54	135	16	47
	20-year (min.)	0	0	0	0	0	0	0	0	0	0
	DSY	0	13	59	106	183	340	85	219	45	130
	ECY	1	5	0	0	0	37	0	44	0	2
	TDY	10	34	42	98	167	298	117	238	25	85
2090s	EWY	80	280	293	437	349	514	512	604	124	216
	20-year (max.)	174	303	289	424	364	535	489	579	164	263
	20-year (avg.)	135	30	47	107	133	271	118	260	38	91
	20-year (min.)	0	0	0	0	37	0	44	0	0	0
	DSY	14	35	39	176	267	376	213	500	64	163

References

- [1] Y. Yau, S. Hasbi, A review of climate change impacts on commercial buildings and their technical services in the tropics, *Renew. Sustain. Energy Rev.* 18 (2013) 430–441.
- [2] S. Liu, Y.-T. Kwok, K. Lau, E. Ng, Applicability of different extreme weather datasets for assessing indoor overheating risks of residential buildings in a subtropical high-density city, *Build. Environ.* 194 (2021), 107711.
- [3] M. Hamdy, S. Carlucci, P.-J. Hoes, J.L. Hensen, The impact of climate change on the overheating risk in dwellings—a Dutch case study, *Build. Environ.* 122 (2017) 307–323.
- [4] A. Gaur, M.K. Eichenbaum, S.P. Simonovic, Analysis and modelling of surface Urban Heat Island in 20 Canadian cities under climate and land-cover change, *J. Environ. Manag.* 206 (2018) 145–157.
- [5] R. Rahif, D. Amaripadath, S. Attia, Review on time-integrated overheating evaluation methods for residential buildings in temperate climates of Europe, *Energy Build.* 252 (2021), 111463, 2021/12/01.
- [6] O. Edenhofer, *Climate Change 2014: Mitigation of Climate Change*, Cambridge University Press, 2015.
- [7] J. Zou, Y. Yu, J. Liu, J. Niu, K. Chauhan, C. Lei, Field measurement of the urban pedestrian level wind turbulence, *Build. Environ.* 194 (2021), 107713.
- [8] J. Zou, J. Liu, J. Niu, Y. Yu, C. Lei, Convective heat loss from computational thermal manikin subject to outdoor wind environments, *Build. Environ.* 188 (2021), 107469.
- [9] J. Luterbacher, D. Dietrich, E. Xoplaki, M. Grosjean, H. Wanner, European seasonal and annual temperature variability, trends, and extremes since 1500, *Science* (New York, N.Y.) 303 (2004) 1499–1503, 04/01.
- [10] G. Brücker, Vulnerable populations: lessons learnt from the summer 2003 heat waves in Europe, *Euro Surveill.* 10 (7) (2005) 1–2, 6p 551.
- [11] T.E.o.E. Britannica, European heat wave of 2003, Available: <https://www.britannica.com/event/European-heat-wave-of-2003>, 2019.
- [12] R. Bustinza, G. Lebel, P. Gosselin, D. Bélanger, F. Chebana, Health impacts of the July 2010 heat wave in Québec, Canada, *BMC Publ. Health* 13 (1) (2013) 56, 2013/01/21.
- [13] MPNRC, Canada heat wave 2021 temperature, deaths, reason, map, Available: <https://www.mprnrc.org/canada-heat-wave-2021-temperature-deaths-reason-map/>, 2021.
- [14] Canada's changing climate report, Available: www.ChangingClimate.ca/CCCR2019, 2019.
- [15] C.B. Field, V. Barros, T.F. Stocker, Q. Dahe, *Managing the Risks of Extreme Events and Disasters to Advance Climate Change Adaptation: Special Report of the Intergovernmental Panel on Climate Change*, Cambridge University Press, 2012.
- [16] C. Mora, et al., Global risk of deadly heat, *Nat. Clim. Change* 7 (7) (2017) 501–506.
- [17] N.E. Klepeis, et al., The National Human Activity Pattern Survey (NHAPS): a resource for assessing exposure to environmental pollutants, *J. Expo. Sci. Environ. Epidemiol.* 11 (3) (2001) 231–252.
- [18] A. Pisello, et al., Test rooms to study human comfort in buildings: a review of controlled experiments and facilities, *Renew. Sustain. Energy Rev.* 149 (2021), 111359.
- [19] C. Shu, et al., Added value of convection permitting climate modelling in urban overheating assessments, *Build. Environ.* 207 (2022), 108415.
- [20] L. Ji, A. Laouadi, C. Shu, A. Gaur, M. Lacasse, L.L. Wang, Evaluating approaches of selecting extreme hot years for assessing building overheating conditions during heatwaves, *Energy Build.* (2021), 111610.
- [21] A. Cripps, P. Wilkinson, M. Davies, M. Orme, *Investigation into Overheating in Homes: Literature Review*, 2012.
- [22] M. Adlington, B. Ceranic, UK care facilities: is climate change contributing to overheating in dwellings and a cause of concern in the health of vulnerable adults, in: *Sustainability in Energy and Buildings 2020*, Springer, 2021, pp. 515–525.
- [23] D. Coley, T. Kershaw, Changes in internal temperatures within the built environment as a response to a changing climate, *Build. Environ.* 45 (2010) 89–93, 01/31.
- [24] S. Kovats, S. Hajat, Heat stress and public health: a critical review, *Annu. Rev. Publ. Health* 29 (2008) 41–55, 02/01.
- [25] P. Acharya, B. Boggess, K. Zhang, Assessing heat stress and health among construction workers in a changing climate: a review, *Int. J. Environ. Res. Publ. Health* 15 (2) (2018) 247.
- [26] D.J. Buysse, R. Grunstein, J. Horne, P. Lavie, Can an improvement in sleep positively impact on health? *Sleep Med. Rev.* 14 (6) (2010) 405–410.
- [27] Y. Wang, Y. Liu, C. Song, J. Liu, Appropriate indoor operative temperature and bedding micro climate temperature that satisfies the requirements of sleep thermal comfort, *Build. Environ.* 92 (2015) 20–29.
- [28] K. Vimalanathan, T.R. Babu, The effect of indoor office environment on the work performance, health and well-being of office workers, *J. environ. health sci. eng.* 12 (1) (2014) 1–8.
- [29] S. Tham, R. Thompson, O. Landeg, K. Murray, T. Waite, Indoor temperature and health: a global systematic review, *Publ. Health* 179 (2020) 9–17.
- [30] F. Lima, P. Ferreira, V. Leal, A review of the relation between household indoor temperature and health outcomes, *Energies* 13 (11) (2020) 2881.
- [31] D.H. Li, L. Yang, J.C. Lam, Impact of climate change on energy use in the built environment in different climate zones—a review, *Energy* 42 (1) (2012) 103–112.
- [32] V. Tink, S. Porritt, D. Allison, D. Loveday, Measuring and mitigating overheating risk in solid wall dwellings retrofitted with internal wall insulation, *Build. Environ.* 141 (2018) 247–261.
- [33] J. Morey, A. Beizaei, A. Wright, An investigation into overheating in social housing dwellings in central England, *Build. Environ.* 176 (2020), 106814.
- [34] S.M.T. Sameni, M. Gaterell, A. Montazami, A. Ahmed, Overheating investigation in UK social housing flats built to the Passivhaus standard, *Build. Environ.* 92 (2015) 222–235.
- [35] I. Pollet, S. Germonpré, A. Vens, Residential ventilative cooling in national energy performance regulations: properties and impact on energy consumption and overheating, in: *Healthy Buildings Europe 2015*, International Society of Indoor Air Quality and Climate (ISIAQ), 2015.
- [36] T. van Hooff, B. Blocken, H. Timmermans, J. Hensen, Analysis of the predicted effect of passive climate adaptation measures on energy demand for cooling and heating in a residential building, *Energy* 94 (2016) 811–820.
- [37] A. Dodo, L. Gustavsson, F. Bonakdar, Effects of future climate change scenarios on overheating risk and primary energy use for Swedish residential buildings, *Energy Proc.* 61 (2014) 1179–1182.
- [38] A. Dodo, L. Gustavsson, Energy use and overheating risk of Swedish multi-storey residential buildings under different climate scenarios, *Energy* 97 (2016) 534–548.
- [39] F.M. Baba, H. Ge, Overheating risk of a single-family detached house built at different ages under current and future climate in Canada, in: *E3S Web of Conferences*, 172, EDP Sciences, 2020, 02004.
- [40] A. Laouadi, M. Bartko, A. Gaur, M.A. Lacasse, Climate resilience buildings: guideline for management of overheating risk in residential buildings, in: *Climate Resilient Buildings and Core Public Infrastructure Initiative (National Research Council of Canada. Construction)*; No. CRBCPI-Y4-10, National Research Council of Canada, 2021. Construction2021/04/01.
- [41] C. Tam, Y. Zhao, Z. Liao, L. Zhao, Mitigation strategies for overheating and high carbon dioxide concentration within institutional buildings: a case study in Toronto, Canada, *Buildings* 10 (7) (2020) 124.
- [42] J.C. Gamero-Salinas, A. Monge-Barrio, A. Sánchez-Ostiz, Overheating risk assessment of different dwellings during the hottest season of a warm tropical climate, *Build. Environ.* 171 (2020), 106664.
- [43] R.-L. Hwang, T.-P. Lin, F.-Y. Lin, Evaluation and mapping of building overheating risk and air conditioning use due to the urban heat island effect, *J. Build. Eng.* 32 (2020), 101726.
- [44] S. Liu, Y.T. Kwok, K.K.-L. Lau, W. Ouyang, E. Ng, Effectiveness of passive design strategies in responding to future climate change for residential buildings in hot and humid Hong Kong, *Energy Build.* 228 (2020), 110469.
- [45] A. Laouadi, M. Bartko, M. Lacasse, A new methodology of evaluation of overheating in buildings, *Energy Build.* 226 (2020), 110360.
- [46] V.M. Nik, Making energy simulation easier for future climate—Synthesizing typical and extreme weather data sets out of regional climate models (RCMs), *Appl. Energy* 177 (2016) 204–226.
- [47] K.E. Taylor, R.J. Stouffer, G.A. Meehl, An overview of CMIP5 and the experiment design, *Bull. Am. Meteorol. Soc.* 93 (4) (2012) 485–498.
- [48] I. Hall, R. Prairie, H. Anderson, E. Boes, Generation of a Typical Meteorological Year, Sandia Labs., Albuquerque, NM (USA), 1978.
- [49] A.L. Chan, T.-T. Chow, S.K. Fong, J.Z. Lin, Generation of a typical meteorological year for Hong Kong, *Energy Convers. Manag.* 47 (1) (2006) 87–96.
- [50] Y. Jiang, Generation of typical meteorological year for different climates of China, *Energy* 35 (5) (2010) 1946–1953.
- [51] H. Li, Y. Yang, K. Lv, J. Liu, L. Yang, Compare several methods of select typical meteorological year for building energy simulation in China, *Energy* 209 (2020), 118465.
- [52] O.S. Ohunakin, M.S. Adaramola, O.M. Oyewola, R.O. Fagbenle, Generation of a typical meteorological year for north-east, Nigeria, *Appl. Energy* 112 (2013) 152–159.
- [53] D. Pissimanis, G. Karras, V. Notaridou, K. Gavria, The generation of a “typical meteorological year” for the city of Athens, *Sol. Energy* 40 (5) (1988) 405–411.
- [54] S. Pusat, İ. Ekmekçi, M.T. Akkoyunlu, Generation of typical meteorological year for different climates of Turkey, *Renew. Energy* 75 (2015) 144–151.
- [55] J. Heckenbergerová, P. Musilek, K. Filimonenkov, Quantification of gains and risks of static thermal rating based on typical meteorological year, *Int. J. Electr. Power Energy Syst.* 44 (1) (2013) 227–235.
- [56] A. Brambilla, J. Bonvin, F. Flourentzou, T. Jusselme, On the influence of thermal mass and natural ventilation on overheating risk in offices, *Buildings* 8 (4) (2018) 47.
- [57] S.C.M. Hui, C. Lok, Test reference year for comparative energy study, *Hong Kong Eng.* 20 (1992) 13–16, 02/01.
- [58] W. Marion, K. Urban, *Users Manual for Radiation Data Base TMY2s Derived from the 1961–1990 National Solar*, National Renewable Energy Laboratory, 1995.
- [59] D.B. Crawley, Which weather data should you use for energy simulations of commercial buildings? *Transact. Am. soc. heat. refrig. air condition. eng.* 104 (1998) 498–515.
- [60] ASHRAE, *International Weather for Energy Calculations (IWEA Weather Files) User's Manual*, ASHRAE, 2002.
- [61] ASHRAE, *Weather Year for Energy Calculations*, American Society of Heating, Refrigerating and Air-Conditioning Engineers, 1985.
- [62] G. Levermore, J. Parkinson, Analyses and algorithms for new test reference years and design summer years for the UK, *Build. Serv. Eng. Technol.* 27 (4) (2006) 311–325.
- [63] T. Hong, W.-K. Chang, H.-W. Lin, A fresh look at weather impact on peak electricity demand and energy use of buildings using 30-year actual weather data, *Appl. Energy* 111 (2013) 333–350.

- [64] M.F. Jentsch, M.E. Eames, G.J. Levermore, Generating near-extreme Summer Reference Years for building performance simulation, *Build. Serv. Eng. Technol.* 36 (6) (2015) 701–727.
- [65] A. Laouadi, A. Gaur, M. Lacasse, M. Bartko, M. Armstrong, Development of reference summer weather years for analysis of overheating risk in buildings, *J. Build. Perfor. Simul.* 13 (3) (2020) 301–319.
- [66] L. Ji, A. Laouadi, C. Shu, A. Gaur, M. Lacasse, L.L. Wang, Evaluating approaches of selecting extreme hot years for assessing building overheating conditions during heatwaves, *Energy Build.* 254 (2022), 111610.
- [67] V.M. Nik, Application of typical and extreme weather data sets in the hygrothermal simulation of building components for future climate—A case study for a wooden frame wall, *Energy Build.* 154 (2017) 30–45.
- [68] A. Moazami, V.M. Nik, S. Carlucci, S. Geving, Impacts of future weather data typology on building energy performance—Investigating long-term patterns of climate change and extreme weather conditions, *Appl. Energy* 238 (2019) 696–720.
- [69] A. Perera, V.M. Nik, D. Chen, J.-L. Scartezzini, T. Hong, Quantifying the impacts of climate change and extreme climate events on energy systems, *Nat. Energy* 5 (2) (2020) 150–159.
- [70] C. Bylund Melin, C.-E. Hagentoft, K. Holl, V.M. Nik, R. Kilian, Simulations of moisture gradients in wood subjected to changes in relative humidity and temperature due to climate change, *Geosciences* 8 (10) (2018) 378.
- [71] M. Hosseini, K. Javanroodi, V.M. Nik, High-resolution Impact Assessment of Climate Change on Building Energy Performance Considering Extreme Weather Events and Microclimate—Investigating Variations in Indoor Thermal Comfort and Degree-Days, *Sustainable Cities and Society*, 2021, 103634.
- [72] Population and Dwelling Count Highlight Tables, 2016 Census, Available: <https://www12.statcan.gc.ca/census-recensement/2016/dp-pd/lt-fst/pd-pl/Table.cfm?Lang=Eng&T=801&SR=1&S=3&O=D&RPP=25&PR=0&CMA=0#tPopDwell, 2018>.
- [73] Canadian climate normals, Available: https://climate.weather.gc.ca/climate_normals/index_e.html, 2021.
- [74] CORDEX, Coordinated regional downscaling experiment (CORDEX) program, Available: <https://cordex.org>, 2021.
- [75] F. Giorgi, C. Jones, G.R. Asrar, Addressing climate information needs at the regional level: the CORDEX framework, *World Meteorol. Organ. Bull.* 58 (3) (2009) 175.
- [76] M.A. Giorgetta, et al., Climate and carbon cycle changes from 1850 to 2100 in MPI-ESM simulations for the Coupled Model Intercomparison Project phase 5, *J. Adv. Model. Earth Syst.* 5 (3) (2013) 572–597.
- [77] N.C. Centre, WCRP CMIP5: Norwegian Climate Centre (NCC) NorESM1-M model output collection, Available: <http://catalogue.ceda.ac.uk/uuid/753310df96fa4d9ca74dd33b19bf330>, 2017.
- [78] M.O.H. Centre, WCRP CMIP5: met office Hadley Centre (MOHC) HadGEM2-ES model output collection, Available: <http://catalogue.ceda.ac.uk/uuid/216becee8a6844ba8a8f8f98b9f075a635>, 2012.
- [79] D. Jacob, R. Poduzin, Sensitivity studies with the regional climate model REMO, *Meteorol. Atmos. Phys.* 63 (1) (1997) 119–129.
- [80] G. Wayne, Representative concentration pathways, *Skept. sci.* 24 (2014).
- [81] D.P. Van Vuuren, et al., The representative concentration pathways: an overview, *Climatic Change* 109 (1) (2011) 5–31.
- [82] E.a.C.C. Canada, Engineering Climate Datasets, 2021.
- [83] D. Maraun, Bias correcting climate change simulations—a critical review, *Curr. Clim. Change Rep.* 2 (4) (2016) 211–220.
- [84] H. Von Storch, F.W. Zwiers, *Statistical Analysis in Climate Research*, Cambridge university press, 2002.
- [85] C. Teutschbein, J. Seibert, Bias correction of regional climate model simulations for hydrological climate-change impact studies: review and evaluation of different methods, *J. hydrol.* 456 (2012) 12–29.
- [86] Y. Hui, J. Chen, C.Y. Xu, L. Xiong, H. Chen, Bias nonstationarity of global climate model outputs: the role of internal climate variability and climate model sensitivity, *Int. J. Climatol.* 39 (4) (2019) 2278–2294.
- [87] A. Gaur, S.P. Simonovic, Towards reducing climate change impact assessment process uncertainty, *Environ. Proces.* 2 (2) (2015) 275–290.
- [88] A. Gaur, M. Lacasse, M. Armstrong, Climate data to undertake hygrothermal and whole building simulations under projected climate change influences for 11 Canadian cities, *Data* 4 (2) (2019) 72.
- [89] C. Piani, et al., Statistical bias correction of global simulated daily precipitation and temperature for the application of hydrological models, *J. hydrol.* 395 (3–4) (2010) 199–215.
- [90] S. Watanabe, S. Kanae, S. Seto, P.J.F. Yeh, Y. Hirabayashi, T. Oki, Intercomparison of bias-correction methods for monthly temperature and precipitation simulated by multiple climate models, *J. Geophys. Res. Atmos.* 117 (D23) (2012).
- [91] P. Berg, H. Feldmann, H.-J. Panitz, Bias correction of high resolution regional climate model data, *J. Hydrol.* 448 (2012) 80–92.
- [92] D. Bannister, et al., Bias correction of high-resolution regional climate model precipitation output gives the best estimates of precipitation in Himalayan catchments, *J. Geophys. Res. Atmos.* 124 (24) (2019) 14220–14239.
- [93] R. Leander, T.A. Buishand, Resampling of regional climate model output for the simulation of extreme river flows, *J. Hydrol.* 332 (3–4) (2007) 487–496.
- [94] H. Li, J. Sheffield, E.F. Wood, Bias correction of monthly precipitation and temperature fields from Intergovernmental Panel on Climate Change AR4 models using equidistant quantile matching, *J. Geophys. Res. Atmos.* 115 (D10) (2010).
- [95] M. Ashfaq, L.C. Bowling, K. Cherkauer, J.S. Pal, N.S. Diffenbaugh, Influence of climate model biases and daily-scale temperature and precipitation events on hydrological impacts assessment: a case study of the United States, *J. Geophys. Res. Atmos.* 115 (D14) (2010).
- [96] A.J. Cannon, Multivariate quantile mapping bias correction: an N-dimensional probability density function transform for climate model simulations of multiple variables, *Clim. Dynam.* 50 (1) (2018) 31–49.
- [97] A.J. Cannon, Multivariate bias correction of climate model output: matching marginal distributions and intervariable dependence structure, *J. Clim.* 29 (19) (2016) 7045–7064.
- [98] A. Gaur, N. Bénichou, M. Armstrong, F. Hill, Potential future changes in wildfire weather and behavior around 11 Canadian cities, *Urban Clim.* 35 (2021), 100735.
- [99] A. Gaur, H. Lu, M. Lacasse, H. Ge, F. Hill, Future projected changes in moisture index over Canada, *Build. Environ.* 199 (2021), 107923.
- [100] V.M. Nik, A.S. Kalagasisid, E. Kjellström, Statistical methods for assessing and analysing the building performance in respect to the future climate, *Build. Environ.* 53 (2012) 107–118.
- [101] V.M. Nik, *Climate Simulation of an Attic Using Future Weather Data Sets—Statistical Methods for Data Processing and Analysis*, Chalmers Tekniska Hogskola, Sweden, 2010.
- [102] CIBSE, *Weather, Solar and Illuminance Data CIBSE Guide J*, Chartered Institution of Building Services Engineers, London, 2002.
- [103] J. Hacker, S.E. Belcher, A. White, Design Summer Years for London, 2014, 05/01.
- [104] D.B. Crawley, et al., EnergyPlus: creating a new-generation building energy simulation program, *Energy Build.* 33 (4) (2001) 319–331.
- [105] J. Boland, B. Ridley, B. Brown, Models of diffuse solar radiation, *Renew. Energy* 33 (4) (2008) 575–584.
- [106] National building Code of Canada 2015, Available: <https://nrc.canada.ca/en/ce/rtifications-evaluations-standards/codes-canada/codes-canada-publications/national-building-code-canada-2015>, 2015.
- [107] P.O. Fanger, Thermal comfort. Analysis and applications in environmental engineering, *Thermal comfort. Anal. appl. environ. eng.* (1970).
- [108] E. 15251, Indoor environmental input parameters for design and assessment of energy performance of buildings addressing indoor air quality, *Thermal Environ. Light. Acoust.* (2007).
- [109] Ergonomics of the thermal environment, Analytical Determination and Interpretation of Thermal Comfort Using Calculation of the PMV and PPD Indices and Local Thermal Comfort Criteria, third ed., 2005.
- [110] R. American Society of Heating and E. Air-Conditioning, *ASHRAE Standard Thermal Environmental Conditions for Human Occupancy*, The Society, Atlanta, Ga, 1992. ©1992, 1992.
- [111] CIBSE, *TM36: Climate Change and the Internal Environment*, 2005.
- [112] CIBSE, "The limits of thermal comfort: avoiding overheating in European buildings," in "TM52," Chartered Institute of British Service Engineers 2013.
- [113] M. Hendel, K. Azos-Diaz, B. Tremeac, Behavioral adaptation to heat-related health risks in cities, *Energy Build.* 152 (2017) 823–829.
- [114] D. Robinson, F. Haldi, Model to predict overheating risk based on an electrical capacitor analogy, *Energy Build.* 40 (7) (2008) 1240–1245.
- [115] D. Robinson, F. Haldi, An integrated adaptive model for overheating risk prediction, *J. Build. Perfor. Simul.* 1 (1) (2008) 43–55.
- [116] V. Goncalves, Y. Ogunjimi, Y. Heo, Scrutinizing modeling and analysis methods for evaluating overheating risks in passive houses, *Energy Build.* 234 (2021), 110701.